Summer 2024

Exploring the Impact of P2Y2 Receptor Activation and Inflammation on Glucose Homeostasis in Mice

Jamila Makhloufi
Missouri State University, Makhloufi612@live.missouristate.edu

EXPLORING THE IMPACT OF $P2Y_2$ RECEPTOR ACTIVATION AND INFLAMMATION ON GLUCOSE HOMEOSTASIS IN MICE

A Master's Thesis

Presented to

The Graduate College of

Missouri State University

In Partial Fulfillment

Of the Requirements for the Degree

Master of Science, Cell and Molecular Biology

By

Jamila Makhloufi

August 2024

EXPLORING THE IMPACT OF $P2Y_2$ RECEPTOR ACTIVATION AND INFLAMMATION ON GLUCOSE HOMEOSTASIS IN MICE

Biomedical Sciences

Missouri State University, August 2024

Master of Science

Jamila Makhloufi

ABSTRACT

Insulin resistance is the body's impaired ability to utilize endogenous and exogenous insulin to take up blood glucose and is associated with many clinical conditions including type 2 diabetes, hypertension, obesity, and cardiovascular disease. The cause of insulin resistance is still unknown; however, it is linked to inflammation. The activation of the purinergic $P2Y_2$ receptor potentiates an inflammatory response under the pathogenesis of obesity and has adverse effects on glucose metabolism by regulating insulin resistance. The goal of this research is to investigate the effects of $P2Y_2$ receptor activation on the downstream signaling pathways of the insulin receptor and glucose uptake. To determine if effects on glucose uptake are specific to the $P2Y_2$ receptor, glucose tolerance testing (GTT) was performed in mice injected with UTP, a P2Y2 receptor ligand, and LPS, a potent activator of the inflammatory response. Glucose tolerance of male and female mice is increased when inflammation is induced by LPS. Male wildtype, but not $P2Y_2$R knockout mice, display a reduced glucose tolerance in the presence of UTP but this effect is not observed in the presence of LPS. These effects seem to be primarily due to regulation of baseline glucose homeostasis rather than a response to challenge, as the effects are no longer present when normalized to baseline, fasting blood glucose levels. We also measured glucose transporter and insulin receptor gene expression and found no significant differences in their expression caused by inflammation or receptor activation. This research suggests that the effects of $P2Y_2$ receptor on glucose homeostasis are minimal, confined to males, and eliminated during acute inflammation.

KEYWORDS: glucose homeostasis, glucose tolerance, inflammation, purinergic receptors,

EXPLORING THE IMPACT OF $P2Y_2$ RECEPTOR ACTIVATION AND INFLAMMATION ON GLUCOSE HOMEOSTASIS IN MICE

By

Jamila Makhloufi

A Master's Thesis
Submitted to the Graduate College
Of Missouri State University
In Partial Fulfillment of the Requirements
For the Degree of Master of Science, Cell and Molecular Biology

August 2024

Approved:

Randi Ulbricht, Ph.D., Thesis Committee Chair

Jianjie Wang, M.D., Ph.D., Committee Member

Scott Zimmerman, Ph.D., Committee Member

Julie Masterson, Ph.D., Dean of the Graduate College

TABLE OF CONTENTS

LIST OF TABLES

LIST OF FIGURES

INTRODUCTION

Glucose is a vital source of energy for most cells in the Human body and is involved in many biochemical processes. Cells and tissues absorb circulating glucose from the blood. Preserving stable blood glucose levels requires coordination between major endocrine organs and metabolic tissues such as the muscle, adipose tissue, liver, and pancreas. In conditions like type 2 diabetes, glucose homeostasis is dysregulated. Type 2 diabetes is marked by chronic hyperglycemia and insulin resistance. Type 2 diabetes is also a major contributor to other comorbidities including cardiovascular disease, hypertension, and high cholesterol. Furthermore, conditions associated with chronic inflammation such as diet induced obesity and cardiovascular disease are also linked to diabetes and glucose dysregulation. This study aims to clarify some of the cellular processes underlying the link between glucose dysregulation and inflammation.

Glucose and insulin regulation

Regulation of blood glucose balance is predominately controlled by the pancreatic endocrine hormones, glucagon and insulin. These hormones are secreted from the pancreas in response to fluctuations in blood glucose concentrations. Insulin is secreted from the islets of Langerhans in pancreatic β-cells in response to increased levels of circulating blood glucose. The insulin binds to the insulin receptor on the target cell and stimulates the uptake of glucose from the blood stream and into the cells, reducing blood glucose[1]. When blood glucose is low, glucagon is secreted from the alpha cells of the pancreas in response to low concentrations of blood glucose. Glucagon stimulates hepatocytes to breakdown and release glucose from the glycogen stores, increasing blood glucose levels. The release of insulin and glucagon, and

subsequent downstream signaling pathways are critical in maintaining balanced levels of glucose in the bloodstream[1] (Figure 1).

Insulin secretion and insulin receptor stimulation in glucose uptake

Following a natural rise in blood glucose concentrations, like eating a meal, increased levels of blood glucose trigger the release of insulin from the β-cells of the pancreas. The circulating insulin binds to the insulin receptor on the membrane surface of peripheral tissues and triggers a signaling cascade[1]. Insulin receptor is a member of the tyrosine kinase family of transmembrane receptors. When insulin binds to the extracellular ligand-binding domain of the receptor, the tyrosine kinase on the intracellular domain becomes auto-phosphorylated. Following receptor activation, the insulin receptor substrate (IRS-1/2) bound to the insulin receptor becomes phosphorylated. Once phosphorylated, the IRS isoform can go on to activate one of two pathways. The first pathway is the mitogen activated protein kinase (MAPK) signaling pathway. The other pathway that promotes glucose uptake from the bloodstream by the cell is the phosphoinositide 3 kinase (PI3K) pathway[2]. In the PI3K pathway, IRS-1/2 forms a complex with PI3K and that causes the phosphorylation of phosphatidylinositol 4,5 bisphosphate (PIP2) to produce phosphatidylinositol 3,4,5 triphosphate (PIP3). PIP3 activates protein 3-phosphoinositidedependent protein kinase-1 (PDK-1) which will then activate protein kinase B (PKB), or AKT. AKT activates the intracellular vesicles storing the glucose transporters and allows them to deposit the stored glucose transporters on to the membrane of the cell. Glucose is then absorbed into the peripheral tissues through transporters, subsequently decreasing blood glucose concentrations[2,3]. AKT also inhibits the activation of glycogen synthase kinase 3 (GSK3) a serine/threonine kinase whose main function is to activate glycogen synthase (GS), creating

glycogen from circulating plasma glucose[4] (Figure 2). Inhibiting glycogen synthesis allows the use the absorbed glucose for energy rather than storing it for use at a later time[5].

Glucose transporters and GLUT4

Glucose transporters (GLUTs) have three distinguished classes: Class I, Class II, and Class III facilitative glucose transporters. Class I facilitative glucose transporters include GLUT1-4 and maintain glucose homeostasis through signal transduction, and transportation of glucose, either import or export[6,7]. Class II transporters include GLUT5, GLUT7, GLUT9, and GLUT 11 and mainly function to transport fructose across membranes of small intestines, kidneys and testes[6]. Class III glucose transporters are less characterized but consist of GLUT6, GLUT8, GLUT10, GLUT12, and GLUT13[6]. Class I has a primary function to facilitate glucose transport in response to insulin, therefore, this paper will focus on class I transport. GLUT2 is responsible for sensing glucose concentrations in both the pancreatic beta cells and hepatocytes. GLUT2 has a very large K_m for glucose and manages large bi-directional flow of glucose in hepatocytes and pancreatic beta cells[6–8]. Like GLUT2, GLUT3 and GLUT1 also have a high K_m for glucose. GLUT3 is highly expressed in the brain and on nervous tissue, whereas GLUT1 is mainly expressed on erythrocytes and endothelial cells. Both GLUT1 and GLUT3 allow for a continuous import of glucose to maintain the metabolic demand of the tissues they supply. GLUT4 is the main insulin dependent glucose transporter and is mainly present in skeletal muscle and adipose tissue. Glucose is transported through GLUT4 in response to circulating levels of glucose in the blood stream and metabolic demand of tissue[6,7,9].

Glucose regulation by metabolic tissues

The mechanisms that regulate glucose homeostasis are divided into two states, absorptive and post-absorptive. The absorptive state, also referred to as fed conditions, is characterized by the digestion of complex carbohydrates to produce the monosaccharide glucose. Glucose is absorbed from the lumen of the small intestine across the mucosal wall, where it enters the bloodstream and is absorbed and stored by peripheral tissues. Glucose levels in the bloodstream are regulated by glucose uptake in insulin-dependent skeletal muscle, adipose tissue, and hepatocytes. The post-absorptive state, also referred to as fasting conditions, is characterized by the fall of plasma glucose levels during sleep, fasting, and in between feeding periods. To keep up with the metabolic demands of tissue, glucagon is released by alpha cells in the pancreas and act on the liver to break down stored glycogen to produce glucose in a process called glycogenolysis. Glucagon also promotes gluconeogenesis in the liver, whereby non-carbohydrate precursors are used to produce glucose[10].

Skeletal muscle

Skeletal muscle is the main insulin dependent tissue that is credited with over 80% of exogenous glucose uptake[11]. The process of which glucose is absorbed into skeletal muscle can be divided into three main steps: First, glucose that is circulating the bloodstream is delivered to the interstitial space. Next, glucose is shuttled through the GLUT4 transporters that are translocated on to the skeletal muscle. Finally, hexokinases in the cell irreversibly phosphorylate glucose and mark it as destined for either glycogenesis or glycolysis[11–13]. Glucose in the glycogenesis pathway form glycosidic bonds between each molecule to form glycogen. Despite skeletal muscle storing up to 70% of the body's glycogen, glycogen in the skeletal muscle is unable to undergo glycogenolysis to be used for energy when the plasma glucose levels fall. However, glycogen in the liver can undergo glucogenesis. When the liver stores of glycogen run

out, skeletal muscle synthesizes glucose from non-carbohydrate precursors, such as lactate, pyruvate, and glycerol[10,13]. The glucose products of gluconeogenesis are then transported to through the body and used as energy in the glycolytic pathway.

Adipose tissue

Adipose tissue is also a key regulator of blood glucose balance. Brown adipose tissue is very important for thermoregulation and energy homeostasis in infants; however, its physiological relevance is essentially nonexistent in adults[14]. When there is an excess of glucose in the bloodstream, glucose becomes a substrate for lipogenesis in white adipose tissue, resulting in storage of triglycerides. Insulin acts on white adipose to stimulate the anabolic pathways that take up and store glucose[15]. When plasma glucose levels decrease in the post-absorptive state, triglycerides are metabolized into free fatty acids (FFA), which is then released into the bloodstream along with glycerol to be transported to the liver to act as precursors in gluconeogenesis[15].

Glucose homeostasis disruption

Insulin resistance. Insulin resistance is defined physiologically as the inability of peripheral tissues to respond to normal insulin levels and subsequently require higher than normal insulin levels to maintain adequate glucose uptake[16]. The cells of affected tissues are no longer responsive to insulin binding to its receptor, therefore, glucose uptake by insulin dependent glucose transporters is compromised. Impaired glucose uptake leads to both hyperglycemia and hyperinsulinemia. High levels of glucose and insulin in the blood stream is a precursor to many pathophysiological conditions such as cardiovascular disease, metabolic syndrome, diabetes mellitus, and obesity[17,18].

Diabetes. Diabetes is characterized by chronically increased levels of glucose in the bloodstream and can be subcategorized into type 1 diabetes (T1D), type 2 diabetes (T2D). According to the Center of Disease Control, diabetes is among the fastest growing chronic diseases in America, with about 1.5 million new cases every year. In the 2022, the CDC release the *National Diabetes Report*, the estimated number of individuals living with diabetes has risen to 37.3 million, which accounts for 11.3% of the U.S. population. Of these, 28.7 million have been diagnosed with diabetes in the past, and approximately 8.5 million people have not been diagnosed. In 2017, diabetes was reported to be the seventh leading cause of death where it was reported as the contributing or underlying cause of death on over 270,000 death certificates[19].

Type 1 diabetes. Type 1 diabetes (T1D) is the inability of the pancreas to secrete sufficient amounts of insulin in order to the cells to take up glucose from the blood stream. The absence of insulin inhibits the insulin dependent uptake of blood glucose and results in chronically elevated blood glucose concentrations[20]. Type 1 diabetes is an autoimmune disease in which T cells target and destroy the insulin producing beta cells of the pancreas. T1D is the most common childhood chronic condition with an estimated prevalence 1 in 300 children. Incidence of childhood diabetes is steadily increasing by 2-5% annually[21].

Type 2 diabetes. In adults, the most common category or diabetes is type 2 diabetes (T2D) which affects over 90% of all individuals diagnosed with diabetes[22]. With T2D, there are two interrelated issues: the cells to do not respond to insulin stimulations and the pancreas is producing higher than normal amounts of insulin in an attempt to elicit a cellular response[17]. These two events lead to a disruption in glucose homeostasis and increase in plasma glucose concentrations, resulting in insulin resistance. Excess glucose in the bloodstream can lead to tissue damage and can result in atherosclerosis, retinopathy and nephropathy[23]. Keeping blood

glucose levels in the normal range requires regular assessment of blood glucose levels, management of diet, and insulin monitoring[24].

Disturbances in glucose levels are assessed by measuring a patient's fasting blood glucose levels and response to oral glucose challenge. Patients are instructed to fast overnight and not to eat anything before the time they are scheduled to have their blood glucose measured in a clinic. Fasting blood glucose levels lower than 100 mg/dL is considered normal, 100-125 mg/dL is considered the range for prediabetes, and above 125 mg/dL is indicative of diabetes[25]. Blood glucose levels after a meal are measured using an oral glucose tolerance test (OGTT). After measuring FBG, in oral glucose tolerance testing, patients consume 75 grams of sugar and blood glucose concentrations are measured over a course of two hours. Results of an OGTT lower than 140 mg/dL is considered normal[25]. Blood glucose levels above this level indicate pre-diabetic (140-199 mg/dL) or diabetic (> 200 mg/dL) levels of glucose dysregulation, suggesting a decrease in the body's ability to metabolize glucose[25]. An abnormal fasting blood glucose and OGTT suggests insulin resistance.

In cases of insulin resistance, hyperinsulinemia develops due to the inability of cells to respond to insulin, resulting in a decrease in glucose uptake and subsequent hyperglycemia. Excess glucose in the bloodstream continues to send signals to the β-cells of the pancreas to release insulin in an attempt to lower plasma glucose levels[1,26]. As a result, insulin levels continue to rise along with plasma glucose in a loop of pathophysiological positive feedback. However, β-cells are not able to maintain the continuously increasing demand of insulin, and eventually stop producing insulin, which results in β-cell dysfunction[27]. The exact cause of insulin resistance remains unknown but is suspected to be caused by changes in the molecules of insulin receptor signaling pathway. Delivery of insulin and glucose to peripheral tissues may be

impaired by poor circulation resulting from chronic hyperglycemia and contribute to insulin resistance[28]. High blood glucose can also stimulate inflammation, which affects both the molecular signaling pathway of the insulin receptor and impairs cardiovascular circulation[29]. Conversely, the presence of acute and chronic inflammation can disrupt glucose homeostasis.

Inflammation pathways and glucose homeostasis: acute vs chronic

Glucose homeostasis is proven to be disrupted in cases of acute inflammation such as severe illness and infection where pro-inflammatory molecules are produced, independent of whether the patient has a previous history of diabetes[30–32]. Clinical studies often highlight and evaluate the relationship between insulin resistance and glucose homeostasis and how it is impacted by illness, sepsis, and stress. During infection there is an upregulation in pro-inflammatory molecules that contribute to a decrease in cardiovascular function and circulation. The reduction in circulation leads to impaired transport of glucose and insulin through the vasculature to the peripheral tissues and increase in pro-inflammatory molecules impairs insulin receptor pathway, subsequently facilitating insulin resistance[33–35].

If bacterial infections are not treated, they can result in a drastic inflammatory response and septic shock. Some cases may result in organ failure[36]. Many experimental models in animals use lipopolysaccharide (LPS) as a way to activate the immune system and simulate an acute inflammatory response. LPS is an endotoxin on the surface of the cell wall of gram-negative bacteria and a potent stimulator of the innate immune system[37,38]. LPS binding protein (LBP) attaches to LPS and shuttles it to the extracellular active site of the toll-like receptor 4 (TLR4) on the surface of immune cells, subsequently causing NF-κB translocation into the nucleus where it acts as a transcription factor to initiate the production of inflammatory cytokines. The inflammatory cytokines produced by this process include reactive oxygen

species, interleukin (Il)-6, Il-1β, Il-10, and tumor necrosis factor (TNF)-α. Activation of the TLR4 receptor on immune cells also results in the liberation of nucleotides to the extracellular fluid[30,39,40].

The body's reaction to inflammation and results of increased production of inflammatory molecules provokes the development insulin resistance due to interference of insulin receptor signaling in the peripheral tissues. Under normal physiological conditions, insulin binding to its receptor leads to a tyrosine residue on IRS-1/2 to be phosphorylated. During the pro-inflammatory state and activation of TLR4, and nucleotide receptors, the tyrosine on the IRS-1/2 is not phosphorylated and instead, a serine is phosphorylated. Therefore, instead of activation of AKT by IRS-1/2 and subsequent GLUT4 translocation and clearance of glucose from the blood, glucose uptake by the cell in impaired in the presence of LPS[41,42].

Obesity and type 2 diabetes are tightly correlated to chronic inflammation. Cytokines such as Il-1β, TNF-α, Il-6, and C-reactive protein (CRP) are all elevated in patients with T2D. Il-6 and TNF- α are both derived from adipose and the increase of these circulatory cytokines is linked to the expansion of adipocytes in obesity[94]. The first cytokine linked with insulin resistance in adipose tissue was TNF-α, which inhibits the auto phosphorylation of the insulin receptor[43].

The relationship between metabolic diseases and inflammation has been investigated through experimental studies that use high-fat-diet (HFD) induced obesity in mice[38]. HFD treated mice have increased levels of pro-inflammatory cytokines that modify the immune response and affect insulin sensitivity in metabolic tissues, such as skeletal muscle, liver tissue, pancreatic tissue, and adipose tissue[44–46]. The inhibition of insulin is attributed to an increase in pro-inflammatory cytokines, extracellular nucleotides, and chemokines. Development of the

inflammatory response in HFD is linked to activation of the purinergic receptor, $P2Y_2$. The $P2Y_2R$ is expressed in many tissue types such as adipose tissue, skeletal muscle, bone, liver, and many endothelial cell types including cardiovascular tissue.

Purinergic receptors

Purinergic receptors are a family of transmembrane receptors expressed on the membrane of many mammalian tissues[47]. Purinergic receptors respond to circulating extracellular nucleotides and are classified into two main families, P1 and P2. G protein-coupled P1 receptors (A1, A2A, A2B, and A3) are strictly stimulated by adenosine, while P2 receptors respond to other extracellular nucleotides including ATP, ADP, UTP, and UDP[47,48]. P2 receptors are further divided into P2Y and P2X receptor subfamilies. ATP activates ionotropic P2X receptors (P2X1-7) by binding to the extracellular domain. G-protein coupled P2Y receptors are expressed as eight subtypes, including $P2Y_1$, $P2Y_2$, $P2Y_4$, $P2Y_6$, $P2Y_{11}$, $P2Y_{12}$, $P2Y_{13}$, and $P2Y_{14}$ receptors (Figure 3). ATP activates $P2Y_2$, $P2Y_{11}$ [49]. $P2Y_1$, $P2Y_{12}$, and $P2Y_{13}$ are activated by ADP. $P2Y_2$ and $P2Y_4$ are activated by UTP. $P2Y_6$, and $P2Y_{14}$ are activated by UDP[47,48] . $P2Y_2$ receptors are activated by circulating UTP and ATP and are widely expressed on the cell membranes of the heart, kidneys, and brain, as well as metabolic tissues and cells like adipocytes[50–54].

$P2Y_2$ purinergic receptor

In the mouse genome, he $P2Y_2R$ gene is found on chromosome 7 whereas in the human genome it is housed in chromosome 11[55]. The $P2Y_2R$ is a GPCR with 7 transmembrane helices. The receptor forms intracellular and extracellular loops, an intracellular C-terminus, and an extracellular N-terminus[56]. The $P2Y_2R$ recognizes and binds integrins by the extracellular loop containing arginine-glycine-aspartate (RGD) residues. The C-terminus allows the $P2Y_2R$ to

associate with tyrosine kinases through the Src homology domain (SH3)[57]. When an activator binds to the $P2Y_2R$, the receptor undergoes a change in conformation that allows interaction with the alpha subunits of the G protein, Gq/11, Gi/o, and G12/13. Coupling of Gq/11 and Gi/o activates the PLCβ pathway[58,59]. As a result, DAG and IP3 are produced and causes release of intracellular calcium stores that allow for the entry of extracellular calcium[60]. When the RGD domain binds to integrins, Rho and Rac GTPases become activated by the $P2Y_2R$ association to Gi/o and G12/13[59].

Current literature of $P2Y_2$ in glucose and insulin pathways

Studies investigating the link between $P2Y_2R$ and regulation of glucose homeostasis have increased in frequency as more evidence supporting their connection has emerged. Research shows that insulin sensitivity and glucose regulation is adversely impacted by $P2Y_2$ in human hepatocytes and skeletal muscle, and in mouse models[51,61,62].

Recent research suggests that the $P2Y_2$ receptor negatively impacts glucose metabolism and the development of insulin resistance. Two studies conducted on human skeletal muscle and human HepG2 hepatocytes demonstrate that an increase in the concentration of extracellular nucleotides and an increase in the concentration of blood glucose leads to the activation of $P2Y_2$ receptors and results in the development of insulin resistance[51,62]. Both studies confirmed the expression of $P2Y_2R$ in their respective tissues via RT-PCR, then incubated the tissues in a high concentration of glucose. Both studies propose glucose stimulates ATP secretion from intracellular storage vesicles. An intracellular calcium mobilization assay showed that increased extracellular ATP levels resulted in the activation of the $P2Y_2$ receptor. The activation of the $P2Y_2$ receptor in these conditions resulted in reduced activation of AKT, a vital protein in the

pathway of insulin dependent glucose uptake. In both papers, $P2Y_2$ also increased signaling of a mitogen-activated kinase involved in inflammation and insulin resistance, ERK1/2[51,62]. These papers suggest that insulin-stimulated glucose uptake in these cells is disrupted by the release of ATP in hyperglycemic conditions, activating the $P2Y_2$ receptor and resulting in insulin resistance.

$P2Y_2$ is also implicated in the pathogenesis of high-fat diet (HFD) induced obesity and insulin resistance in recent *in vivo* research. Both studies assessed glucose regulation in $P2Y_2R$ knockout and wildtype HFD fed male mice. Zhang et al. showed that following a high-fat diet, $P2Y_2R$ deficient mice had a decrease in insulin secretion compared to the wildtype mice as well as an increase in the gene expression insulin receptor substrate 1 (IRS-1) and glucose transporter 4 (GLUT4), molecules necessary for insulin-dependent glucose uptake[61]. Another study tested insulin sensitivity following a HFD using C-peptide quantification and an insulin tolerance test[52]. Insulin receptor sensitivity was shown to increase in HFD fed $P2Y_2R$ lacking mice compared to wildtype mice[52]. Both studies support that the $P2Y_2$ receptor plays an important role in the development of insulin resistance in high-fat diet conditions.

Sex specific differences in glucose and insulin regulation

Sex hormones have been found to play pivotal role in regulating glucose metabolism. Studies show that women exhibit higher sensitivity to insulin than men, despite the fact that women, relative to men, also display characteristics known to increase insulin resistance including lower skeletal muscle mass, greater white adipose mas and an increased in free fatty acids[63].

It is reported that the sex differences in insulin sensitivity are correlated with the difference in estrogen levels in men and women[64]. The influence of estrogen in sex dependent

gluce regulation was further studied by Mauvais-Jarvis, observing the changes in estogen levels as women age and how they effect sensitivity to insulin. Post-menopausal women were shown to have a significant decreased in insulin sensitivity compared to pre-menopausal women. Young adult women are also not as succeptible to developing insulin resistance compare to age matched men, however, rates of insulin resistance in post-menopausal women are statistically equivilant to men, suggesting estogen protects against insulin resistance[65].

Sex-dependent glucose regulation is associated with sex hormone-dependent differences in gene expression. One study shows that estrogen functions as a transcription factor in the nucleus by recruiting coactivators that upregulate the expression of genes involved in glucose metabolism, such as GLUT4[66]. Female mice are shown to have increased levels of GLUT4 expression compared to males and have higher levels of AKT phosphorylation following insulin administration[67]. This may contribute to better insulin sensitivity in females due to their higher estrogen levels. Genes unrelated to metabolism also impact glucose homeostasis differently in males and females. For instance, studies on GRK2 in high-fat diet fed mice reveal that young females exhibit lower GRK2 expression and better insulin sensitivity compared to age-matched males and older females[68]. These findings underscore how sex hormones influence gene expression and facilitate sexual dimorphisms of glucose metabolism and the development of insulin resistance.

Sex specific differences in inflammation

There are known differences between males and females in the response to inflammation. Sex hormones have been found to play pivotal role in regulating sex-specific differences in inflammation. Studies show that women exhibit higher sensitivity to chronic inflammation and

are more susceptible to the development of autoimmune diseases. Meanwhile males exhibit a more robust response to acute inflammation[69].

A study comparing male and female human peripheral blood mononuclear cell (PBMC) response to inflammation revealed males have a greater acute response to inflammation than females[70]. Male and female PBMCs were incubated for 6 hours following treatment with 1 ng/mL of lipopolysaccharide (LPS), estradiol, or LPS and estradiol. Male PMBCs secreted more TNF-α while female PBMCs secreted higher levels of IL-6 following LPS treatment. Estradiol resulted in no significant differences in cytokine secretion of female cells, while it increased cytokine secretion in male PBMCs. When cells were treated with both LPS and estradiol, sex differences in LPS-stimulated TNF-α or IL-6 secretion were insignificant, but male PBMCs had an increased secretion on IL-10 compared to female cells[70]. This further supports the findings that estrogens display an anti-inflammatory effect and improve outcomes of acute inflammation[71]. On the other hand, androgens such as testosterone are considered to be both anti-inflammatory as well as immunosuppressive as they reduce the activation of NFκ-b, but also decrease the activity of natural killer cells[72].

Sex specific inflammatory responses are also influenced by mechanisms involving X chromosomes. The X chromosome is known to contain genes responsible for responding to inflammation. One example are the genes responsible for encoding pattern recognition receptors (PRRs)[73]. These receptors recognize damage associated molecular patterns (DAMPs) and pathogen associated molecular patterns (PAMPs)[73,74]. In females, duplicated X genes are inactivated (XCI) to prevent over expression. PRR toll-like receptor 7 (TLR7) is expressed on the X chromosome and if the gene escapes inactivation in one chromosome it will be expression more in females compared to males. Activation of TLR7 increases production of pro-

inflammatory molecules and increases risk of developing autoimmune diseases in females[75,76]. Males, however, exhibit a higher expression of toll-like receptor (TLR4) on macrophages compared to females. TLR4 can be activated by LPS and result in higher levels of chemokines secreted in males relative to females[77]. One study shows that LPS-stimulated pro-inflammatory cytokine production is greater in male mice compared to female mice, however this result is mitigated when androgens were removed from the male mice[78].

Research goal and aims

Glucose homeostasis is complexly regulated by a variety of biological factors that differ between male and female subjects, the exact mechanism of which remains unknown. Research investigating the influence of $P2Y_2$ receptor signaling and the role of inflammation in the ability of the body to regulate glucose metabolism in conjunction with the influence of male and female biological factors is highly limited. The goal of this paper is to investigate the influence of inflammation induced by the $P2Y_2$ receptor on glucose metabolism and insulin resistance in male and female mice. We will use UTP and LPS challenges to determine if activation of the $P2Y_2$ receptor affects glucose homeostasis in the presence of inflammation.

Aim 1: Inject mice with UTP to stimulate $P2Y_2$ and LPS to stimulate inflammation then perform GTT. An intraperitoneal glucose tolerance test (GTT) allows us to evaluate the ability of mice to metabolize glucose. We will perform a GTT after challenging mice with LPS to induce acute inflammation and UTP to activate the $P2Y_2$ receptor.

In previous work, blood glucose levels from LPS treated increased to a greater extent in male mice after glucose challenge, indicating a reduced glucose tolerance, compared to untreated males. Interestingly, this LPS-mediated affect was not present in $P2Y_2R$ knockout animals or in wildtype female mice[79]. This suggests that there is a male specific $P2Y_2R$ mediated effect on

glucose tolerance. In this study, we will add to this model by stimulating the $P2Y_2R$ with UTP, expecting the activation of the receptor to amplify the effects of inflammation in wildtype animals (Figure 4).

Aim 2: Quantify GLUT4 and insulin receptor expression in abdominal muscle tissue. Both GLUT4 and INSR are vital in the uptake and regulation of blood glucose. Male and female hormonal physiology influence many signaling pathways and may regulate glucose homeostasis through the expression of GLUT4 and INSR. We will investigate this possible relationship by dissecting abdominal skeletal muscle from male and female $P2Y_2R$ knockout and wildtype mice and measuring the expression of GLUT4 and INSR via qRT-PCR.

Aim 3: Quantify GLUT4 expression in adipose tissue. Adipose tissue is the main metabolic tissue where glucose is stored. Weight gain and adipose tissue hypertrophy are common complications of insulin resistance and type 2 diabetes. We will investigate possible relationships between GLUT4 expression and insulin resistance by dissecting visceral fat from male and female $P2Y_2R$ knockout and wildtype mice and measure the expression of GLUT4 via qRT-PCR.

Study implications

By examining how glucose is processed and regulated differently between the sexes, this study aims to reveal underlying physiological mechanisms that contribute to divergences. Sexual dimorphisms that influence biological factors governing glucose metabolism are known but not well understood. A sex-specific role for the $P2Y_2$ receptor may help explain sex-specific vulnerabilities to metabolic disorders such as diabetes and obesity. Moreover, it is important to understand how pharmacological targeting of $P2Y_2R$ may differentially affect those experiencing inflammation based on sex. Ultimately, the findings here could give new insights for distinctive

approaches to prevention, diagnosis, and treatment strategies designed specifically for males and females, thereby advancing the precision of medicine.

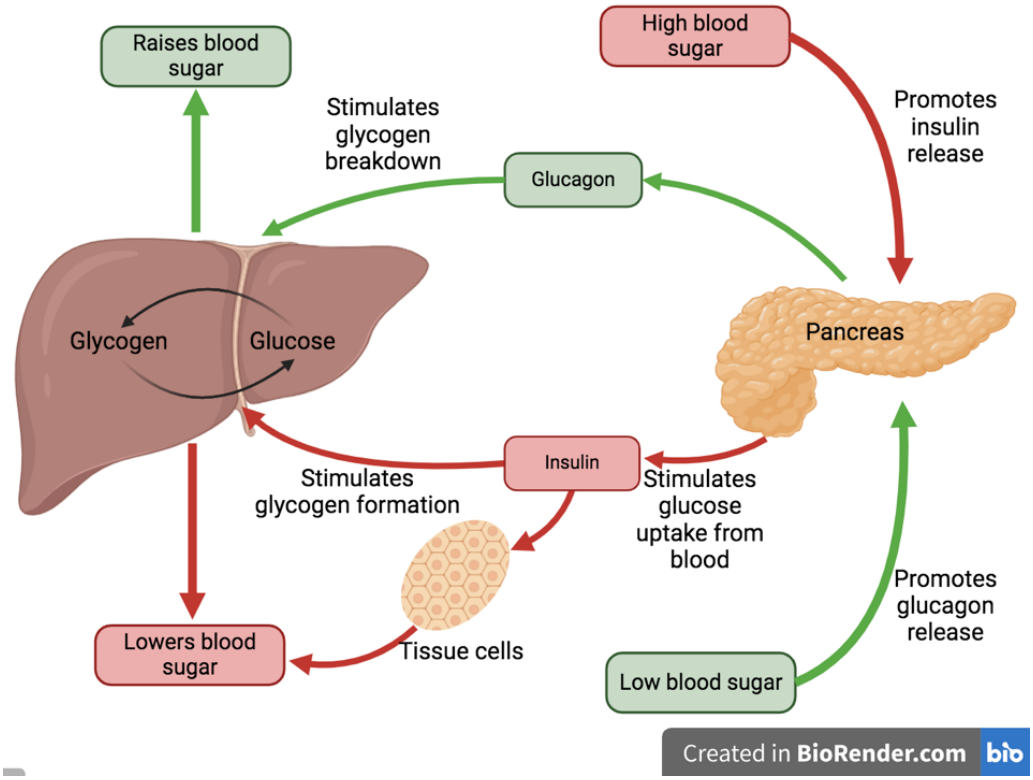

Figure 1. Maintenance of glucose homeostasis. When blood sugar is high (red arrow pathway), the pancreas releases insulin, which results in the stimulation of cells to take up extracellular glucose or the liver converts glucose into glycogen for storage. Both result in lowering blood sugar. When blood sugar levels are low (green arrow pathway), glucagon is released from the pancreas and acts on the liver to promote the breakdown of glycogen into glucose to be release into the bloodstream, thereby raising blood glucose levels.

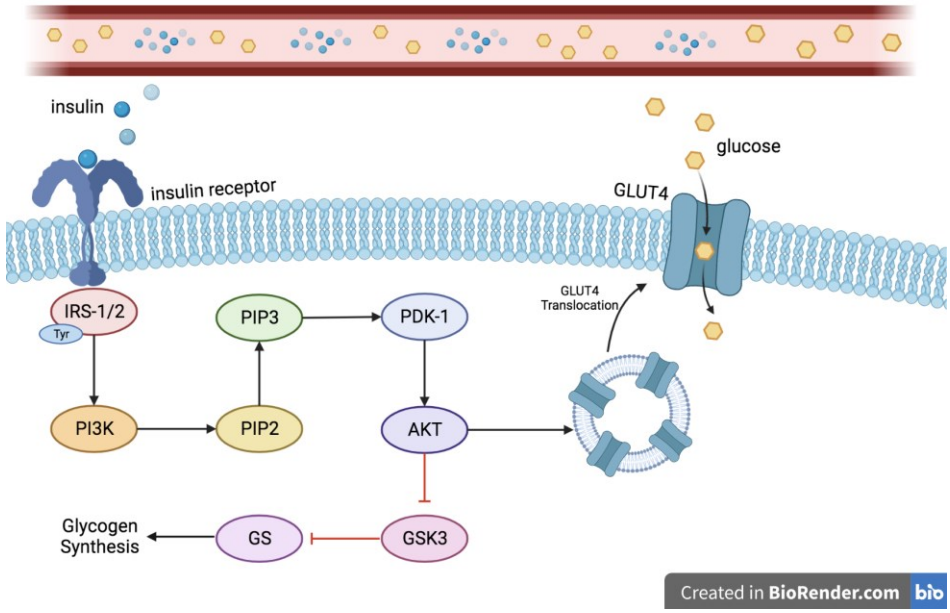

Figure 2. Insulin receptor signaling. Insulin binds to the insulin receptor on insulin-dependent cells and activates the receptor, leading to the phosphorylation of a tyrosine residue on IRS-1/2. IRS-1/2 binds to PI3K which converts PIP2 to PIP3. PIP3 stimulates PDK-1 to phosphorylate AKT which then associates with GLUT4 storage vesicles (GSV), stimulating the translocation of GLUT4 to the membrane surface. GLUT4 enables glucose uptake from the blood stream and into the cell.

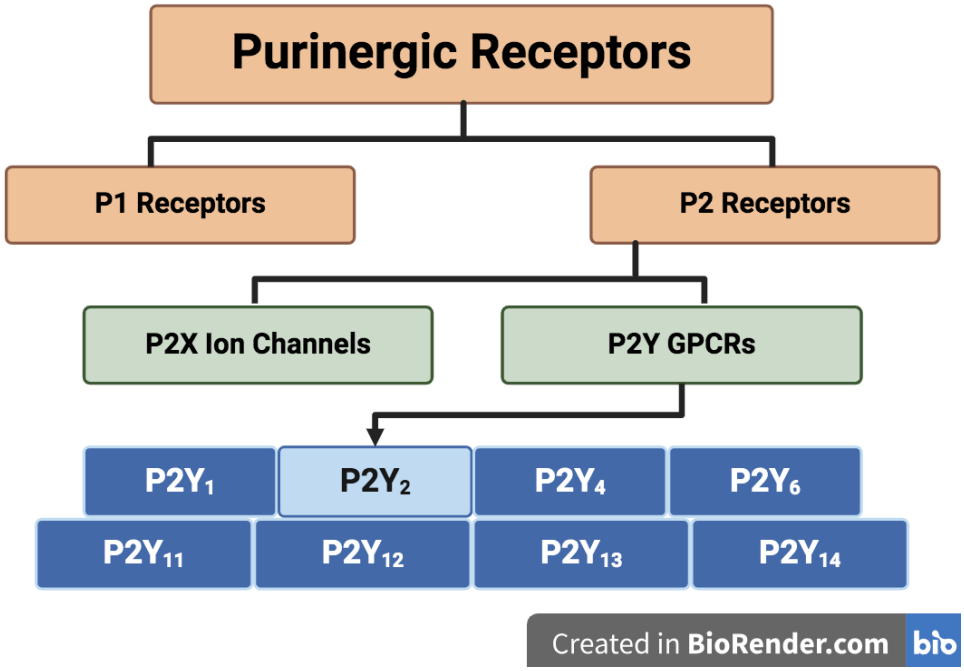

Figure 3. Tree of purinergic preceptors. P2 receptor broken down into P2X ion channels and P2Y GPCRs. Subtypes of P2Y receptors shown with emphasis on $P2Y_2$.

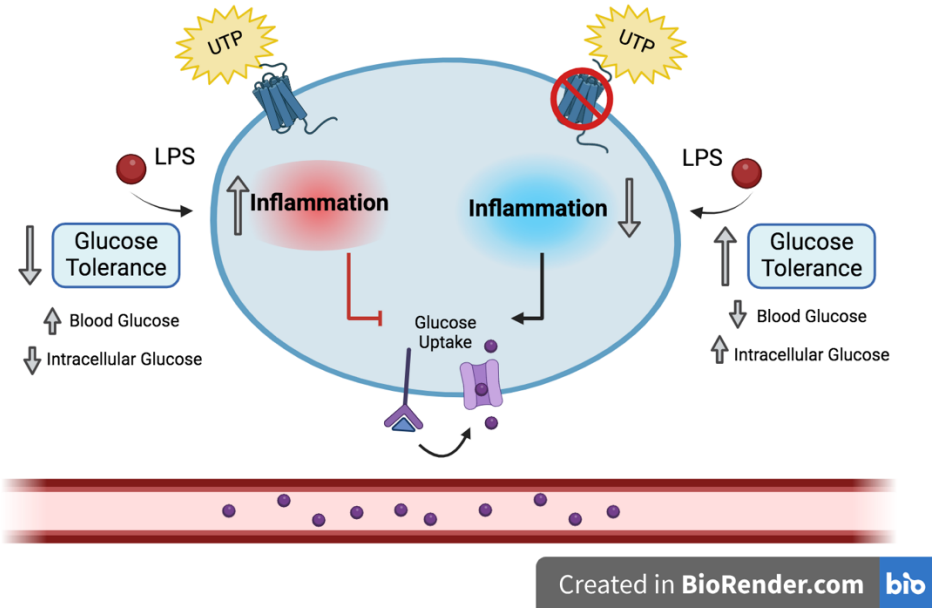

Figure 4. Expectations of research results. In wildtype mice, stimulation with UTP is expected to activate the $P2Y_2$ receptor, heightening the effects of inflammation and attenuate insulin receptor signaling. The expected result is a decrease of glucose tolerance. In $P2Y_2$ knockout mice, stimulation with UTP will not be able to activate the receptor, allowing insulin receptor signaling to increase glucose uptake. The expected result is greater glucose tolerance.

METHODS

All methods performed for this thesis were completed prior to May 2024. Required safety trainings were completed (Appendix A) and the Missouri State University Institutional Animal Care and Use Committee (IACUC) approved all of the procedures performed in this study (Protocol 2021-02, Appendix B). Institutional biosafety committee (IBC) and institutional review board (IRB) approval was not required for this work.

Mice

Heterozygous genetically modified $P2Y_2R$ knockout and wildtype C57BL/6J mice[55] were acquired from The Jackson Laboratory (stock # 009132, Bar Harbour, Maine). The colony was maintained by heterzygous breeding. All mice used in this study (Table 1) were born and housed in Temple Hall vivarium at Missouris State University. Mice were maintained on a 12-hour light-dark cycle, 7 pm-7 am light and 7 am-7 pm dark, at a temperature of 76 °F and a 30-70% humidity. Mice were fed Laboratory Rodent Diet (Purina, catalog #0001319, St. Louis, Missouri). At three weeks old, mice were ear-tagged and genotyped. At seven weeks old, mice were moved to the vivariam in Kampeter Hall of Missouri State University and acclimated for one week. Experiments were performed on mice that were eight to 12 weeks old.

Genotyping

Male and female heterozygous $P2Y_2R$ knockout mice were bred to produce mice used in this study. Heterozygous mating was projected to produce 50 % heterozygous, 25 % wildtype (WT), and 25 % $P2Y_2R$ knockout (KO) offspring. For identification, $\geq$ 2mm of the mouse tail

ends were snipped and added to a sterile tube. The DNA was extracted using the Phire Tissue Direct PCR Kit from Thermo Scientific. Twenty µL of dilution buffer was mixed with one µL of DNA release and added to each tail snip. The tail snips were vortexed to evenly coat them in the DNA release solution and incubated at room temperature for five minutes followed by a three-minute incubation at 95 °C to stop the reaction. Tail snips were vortexed and spun down for 30 seconds to collect the sample at the bottom of the tube.

The presence of the wildtype $P2Y_2R$ gene or knockout allele was determined using PCR. In clear PCR tubes, 2 µL of one tail snip DNA was combined with 10 µL of DreamTaq mastermix (Thermo), 5.6 µL of RNase free water, 160 ng each oligonucleotide primer to total of 20 µL. Three primers were used in each reaction: one is antisense to both the wildtype and knockout $P2Y_2R$, but sense primers will bind only one genotype, producing bands of differing sizes, depending on genotype (Table 2). In the thermocycler, the PCR samples were first held at an initial denaturation step at 95 °C for 2 minutes, followed by a denaturation step at 95 °C for 30 seconds, an annealing step at 60 °C for 30 seconds, and an extension step at 72 °C for 30 seconds. The denaturation, annealing, and extension steps were repeated 37 times, followed by a final extension step at 72 °C for 5 minutes. The PCR product was electrophoresed at 230V for 20-30 minutes on a 2% agarose gel with Ethidium Bromide (EtBr). Gels were prepared and electrophoresed in 1X sodium borate buffer. Genotypes were reported based on the presence of only the wildtype allele (homozygous wildtype, 450 base pairs), only the knockout allele (homozygous knockout, 580 base pairs), or one of each product (heterozygous) (Figure 5).

Intraperitoneal glucose tolerance test

An intraperitoneal glucose tolerance test (GTT) was used to evaluate the ability of the mice to metabolize glucose. Twenty-four hours before beginning the GTT, mice were injected

with LPS from *E.coli* (Sigma, St. Louis, Missouri) at 2 mg/kg or with the same volume per kg of 0.9% saline for control groups. After 19 hours, food from the mouse cages were removed to begin a five hour fast and establish fasting blood glucose levels, while access to water remained ad libitum. Thirty minutes before the GTT, mice were placed in tall Styrofoam boxes with a handwarmer covered by bench paper. The mice were injected with 200 μL of 10^{-4} M UTP per 25 g of body weight, or an equal volume per body weight of 0.9% saline. Lidocaine (Patterson Veterinary, Supply lidocaine HCl 2%, Inc., Kansas City, Missouri) was applied to the tips of the mouse tails for 10-15 minutes for local anesthesia. The distal 2-5mm of the mouse tail was cut off with a sterile surgical blade and fasting blood glucose levels were measured with a glucometer and blood glucose test strips (Walmart, ReliOn, Bentonville, Arkansas). Immediately following fasting blood glucose reading, a dextrose injection of 2 g/kg in 0.9 % saline was administered to each mouse. Blood glucose was then measured at 10, 20, 30, 45, 60, 75, and 90 minutes following the dextrose injection (Figure 6).

Tissue dissections

Immediately following GTT, mice were anesthitized with isofluorane and sacrificed by and cervical dilocation. Abdominal skeletal muscle and visceral adipose tissue were dissected and immediately snap frozen in liquid nortigen and stored at –80 ˚C until RNA extractions.

Quantitative RT-PCR

RNA Isolation. To isolate total RNA from dissected tissues, Ambion TRIzol reagent (catalog #15596018) was added to the tissue samples at 1 mL of cold TRIzol per 100 mg of tissue sample. Tissue samples were homogenized into the reagent using a FisherBrand Ultrasonic Liquid Processor (model #FB-120). For adipose tissue samples, the lysate was centrifuged for 5

minutes at 12,000 x g at 4 ˚C and the clear supernatant was transferred to a new tube. We added 0.2 mL of chloroform per 1 mL o TRIzol to the tube and vortexed. Samples were centrifuged for 15 minutes at 12,000 x g at 4 ˚C and the phase separation was observed. The lower red layer was the inorganic phenol-chloroform followed by the thin white interphase and the top-most colorless layer in the organic aqueous phase. The aqueous phase containing the RNA was carefully removed to not disturb the interphase and placed into a new tube where 0.5 mL of isoproponal was added per 1 mL TRIzol used. The aqueous layer and isopropanol were centrifuged for 10 minutes at 12,000 x g at 4 ˚C to pellet the RNA. After removing the supernatant, the pellet was resuspended to 1 mL of 75% ethanol per 1 mL of TRIzol used. The sample was then centrifuged for five minutes at 7,500 x g at 4 ˚C. The supernatant was discarded using a pipette and the tubes were left open until the RNA had completely dried. The pellet was then resuspended in 50 µL of diethyl pyrocarbonate (DepC) treated water and frozen at –80 ºC.

cDNA synthesis. To synthesize cDNA, we used the Applied Biosystems High Capacity cDNA Reverse Transcription Kit (catalog #4368814). Two mastermixes were prepared using the dNTPs, buffer, random primers and water, however reverse transcriptase was only added to one of the master mixes and the other mix recieved water in its place. One µg of RNA was added to 20 µL of mastermix containing 0.5 X dNTPs, 1 X buffer, 1 X random hexamers, and 1 µL of either reverse transcriptase or water and inclubated for 10 minutes at 24 ˚C, followed by one hour at 37 ˚C and 10 minutes at 85 ˚C.

Quantitative PCR. To determine the relative expression of INSR and GLUT4, the cDNA was subjected to quantitative PCR. cDNA was diluted to 1:10 ratio by adding 5 µL of cDNA to 45 µL of water. Two PCR reaction were made for each sample, two that included reverse transcriptase (+RT), two controls that did not include reverse transcriptase (-RT), and

one reaction with no cDNA (no template, NT) to serve as a control. A 10 µL reaction was prepared with 2 µL of diluted cDNA, 5 µL of iTaq Universal SYBER green mix (Bio-Rad), 100ng of primer (either PPIA, INSR, or GLUT4; Table 1), and 2.5 µL of water. Reaction mixes were subject to qPCR in a CFX connect real-time detection system (BioRad) with an initial step of 2 minutes at 95 ˚C, followed by 5 seconds at 95 ˚C and 30 seconds at 60 ˚C. The 5 second and 30 second steps were repeated 39 more times with a plate read after each cycle. Every qPCR was followed by a melt curve analysis of 65-95 ˚C in increments of 0.5 ˚C with a plate read.

Statistical analysis

All statistical analysis was performed using Jeffrey's Amazing Statistics Program (JASP) (Appendix C).

Glucose tolerance test analysis. ANOVA with repeated measures followed by Tukey-Mann multiple comparisons was used to evaluate GTT raw and normalized data. Error bars represented are reported as Mean ± SEM. Normalized blood glucose values were established by dividing the blood glucose from each individual timepoint by the respective fasting blood glucose of each mouse.

Area under the curve (AUC) was calculated on each individual GTT curve. The average AUC for each condition is presented with error (SEM). The AUC and fasting blood glucose were analyzed by ANOVA with Tukeys multiple comparisons. An outlier test was performed to identify and eliminate outliers from the primary analysis group. Statistical significance was reported as p-value is less than 0.001, 0.01, and 0.05.

Gene expression analysis. The relative gene expression was calculated by using the Ep value to find the fold change (= (Ep)ΔC_T) of the sample, where the ΔC_T was calculated by taking the average of each target C_T and subtracting that from the average C_T of male wildtype

saline control animals[80]. The fold change of the gene of interest (INSR and GLUT4) was divided by the fold change of the housekeeping gene. The housekeeping gene was PPIA, as the experimental variables in this study have no known influence in PPIA expression. A classical ANOVA was used to analyze gene expression and multiple comparisons t-test perperformed to analyze significant differences between the experimental groups. Ratios determined from the Pfaffl method[80] were analyzed for significance by an unpaired t-test.

Table 1. Mice used in this study.

Sex and Genotype	Treatments				Total
	Saline		LPS		
	Saline	UTP	Saline	UTP	
Female WT	3	4	4	5	16
Female $P2Y_2R$ KO	5	6	5	6	22
Male WT	4	3	4	5	16
Male $P2Y_2R$ KO	0	0	0	0	0

Table 2. Primers used in this study.

Primers	Sequence
GLUT4 qRT-PCR	**5'**- TCTTATTGCAGCGCCTGAG -**3'** **5'**- GAGAATACAGCTAGGACCAGTG -**3'**
INSR qRT-PCR	**5'**- TCAATGAGTCAGCCAGTCTTC -**3'** **5'**- CAATTCCATCACTACCAGCGT -**3'**
PPIA qRT-PCR	**5'**- CAAACACAAACGGTTCCCAG -**3'** **5'**- TTCACCTTCCCAAAGACCAC -**3'**
$P2Y_2R$ genotyping	**5'**- AGCCACCCGGCGGGCATAAC -**3'** **5'**- GAGGGGGACGAACTGGGATAC -**3'** **5'**- AAATGCCTGCTCTTTACTGAAGG -**3'**

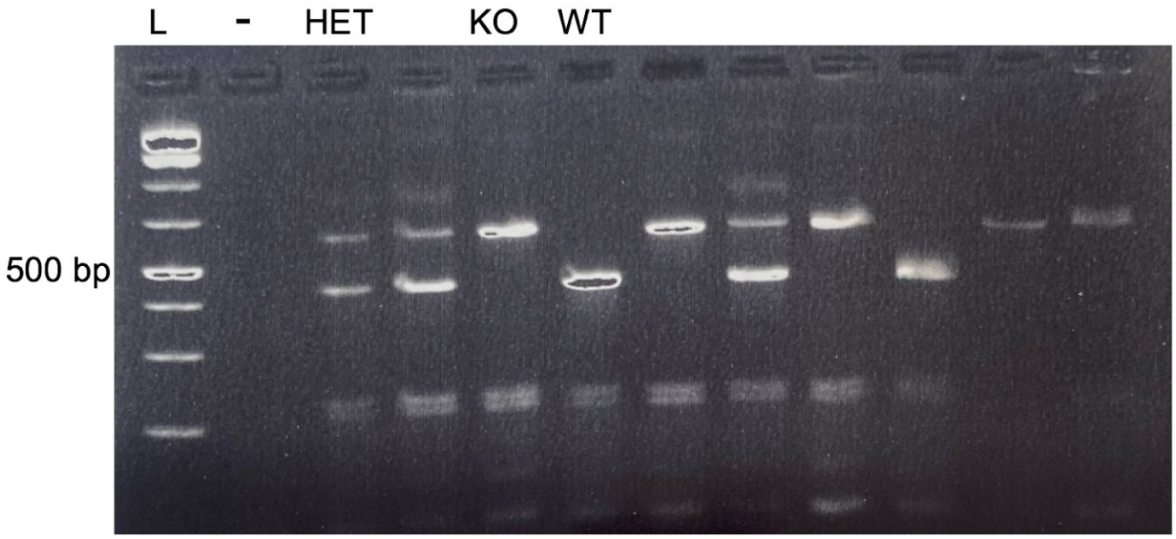

Figure 5. P2Y$_2$R genotyping results. P2Y$_2$R wildtype (WT) and knockout (KO) mouse DNA was amplified by PCR. The PCR products were electrophoresed in 1 X sodium borate buffer on a 2% agarose gel. A 1000 base pair (bp) ladder is shown on the left (L), followed by a negative control containing no DNA (-), and a positive heterozygous (HET) control. The expected band size of P2Y$_2$R knockout mice is 580 bp and for wildtype mice the expected size is 450 bp. HET mice will have bands at 580 and 450 bp.

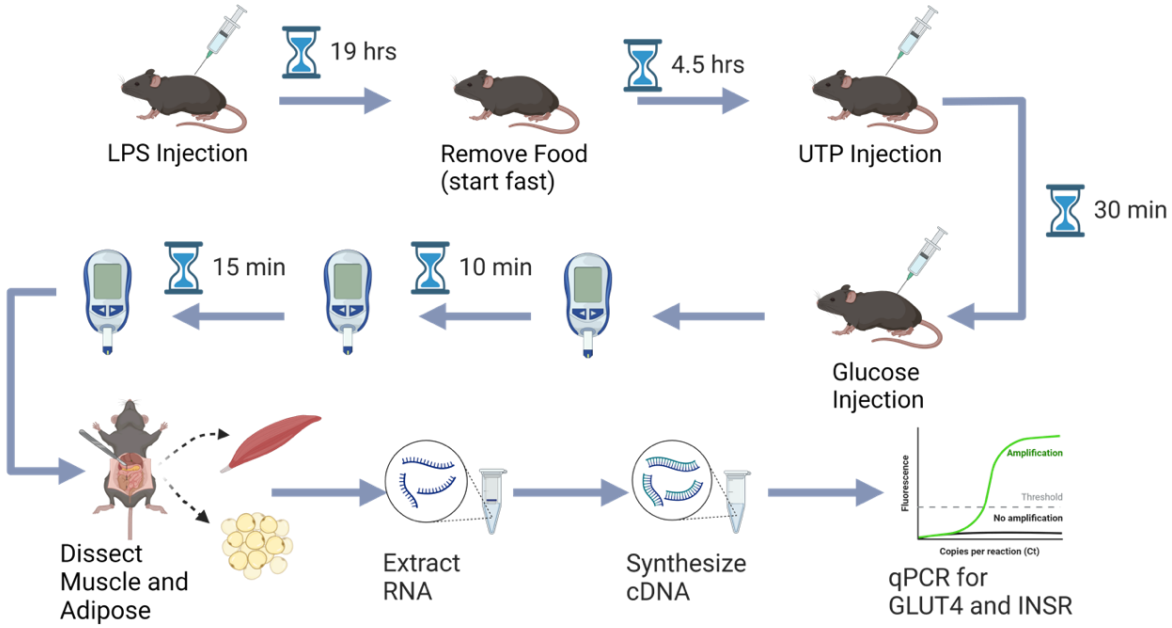

Figure 6. GTT and gene expression methods. Mice received an intraperitoneal injection of LPS or saline. After 19 hours, food was removed from mouse cages while water remained, and mice began a 5 hour fast. Mice received an IP injection of UTP or saline 30 minutes before an IP injection of glucose injection. Blood glucose was determined from tail snip bleeding every 10 min for 30 min, and every 15 min for 60 min (total time 1.5 hours). Mice underwent dissections

for abdominal skeletal muscle and visceral adipose immediately following GTT. RNA was extracted from tissues and used for qRT-PCR to quantify expression of GLUT4 and INSR.

RESULTS

The goal of this thesis is to investigate the influence of inflammation induced by the $P2Y_2$ receptor on glucose metabolism in male and female mice. Glucose metabolism is primarily measured with a glucose tolerance test (GTT). GTT measures the physiological response to glucose and how quickly the cells of the body are able to take up exogenous glucose from the blood stream. The GTT starts by fasting mice for 5 hours, then a glucose injection. Blood glucose is measured over a 90-minute period. We report the raw blood glucose over the course of GTT, the rate of glucose change, the area under each GTT curve, as well as fasting blood glucose levels.

$P2Y_2$ receptor and inflammation effects on fasting blood glucose

This fasting glucose concentration is determined after the mice have been without food for 5 hours, but before the glucose injection. Fasting blood glucose is a measure of the basline metabolic state of the mice. Thirty minutes prior to fasting blood glucose measurements, mice were injected with UTP to stimulate the $P2Y_2R$ receptor. Treatment with UTP does not significantly affect fasting blood glucose in males or females (Figure 7), suggesting that stimulation of the receptor did not alter baseline blood glucose regulation.

We also measured fasting blood glucose levels in mice where the $P2Y_2R$ expression has been eliminated by knocking out the recepter in the genome. We did not have access to male $P2Y_2R$ knockout animals, and therefore were only able to measure fasting blood glucse in $P2Y_2R$ knockout females. Among females, there were no significant differences in fasting blood

glucose between wildtype and knockout ($p = 0.516$, Figure 7). This data, like the UTP data described above, suggests that $P2Y_2R$ does not regulate fasting blood glucose in females.

Twenty-four hours prior to fasting blood glucose measurements, mice were injected with LPS in order to stimulate inflammation. LPS treatment results in lower fasting blood glucose than control saline injection in male ($p < 0.001$) and female mice ($p < 0.001$, Figure 7). This data is consistent with previous studies from our lab, indicating that this dose and timing of LPS reduces blood glucose levels[81].

There were no differences in fasting blood glucose between males and females in our study ($p = 0.607$, Figure 7). This is in contrast to previous data that shows reduced fasting blood glucose in females compared to males[79].

Glucose tolerance test

Over the course of the 90 min GTT, blood glucose concentration should increase immediately following the glucose injection. After a peak blood glucose concentration around 10 min, the glucose levels will decrease as the glucose is absorbed from the blood into the cells. By the end of 90 min, blood glucose should return to baseline, fasting levels. GTT curves were developed by determining the average blood glucose concentration from each group. A decreased glucose level over the course of GTT generally indicates a greater glucose tolerance.

Inflammation in glucose metabolism. Both male and female mice showed a similar and expected trend in the GTT curve where blood glucose levels rose quickly after 0 min until about 10 min. The blood glucose steadily decreased from the peak until they return to the fasting concentration at 90 minutes (Figure 8 and Figure 9). Previous studies have shown that LPS increases glucose tolerance in both male and female mice[79,82,83]. Indeed, the GTT curves were lower throughout the test, indicating that concentration of blood glucose is lower in LPS treated

mice than the control group which is treated with saline instead of LPS ($p < 0.001$, Figure 8 D). In males, LPS treated mice had lower blood glucose concentrations than the control at 10 min ($p < 0.001$), 20 min ($p < 0.05$), 30 min ($p < 0.001$), and 45 min ($p < 0.01$) (Figure 8 B). In female wildtype mice, LPS treatment had lower blood glucose concentrations than the control at 10 min ($p < 0.001$), 20 min ($p < 0.001$), and 30 min ($p < 0.01$) after glucose injection (Figure 8 A). In female $P2Y_2R$ knockout animals, LPS treated mice only had a significantly lower blood glucose concentration at 10 min ($p < 0.001$), while there were no significant differences in the rest of the curves (Figure 8 C).

The area under the curve for GTT represents the total rate of glucose accumulation and clearence. A smaller area under the curve (AUC) represents more efficient clearance of glucose, indicating increased tolerance to glucose. The areas under the curve were lower in the LPS treated animals compared to control animals ($p < 0.001$, Figure 8 D), confirming increased glucose tolerance during inflammation.

Influence of $P2Y_2$ and UTP on glucose metabolism. To assess the role of $P2Y_2$ receptor in glucose metabolism, wildtype and $P2Y_2R$ knockout mice were treated with UTP to stimulate the receptor, then subject to glucose tolerance testing. During GTT, female mice did not display any significant differences in blood glucose concentration between the genotypes (Figure 8). UTP treatment did not affect the AUC in female mice further suggesting that receptor activation does not affect glucose tolerance in females. UTP treated male mice had an increase in blood glucose concentration from 10 to 45 min after glucose injection compared to other male treatment groups($p < 0.001$, $p < 0.013$, $p < 0.01$, $p < 0.009$, respectively; Figure 8 C). UTP treatment of wildtype male mice had an overall greater AUC than the control group ($p < 0.001$,

Figure 8 D). Together, these results suggest that purinergic receptor activation decreases glucose tolerance in male mice only, but only in conditions without LPS.

Influence of sex in glucose metabolism. Throughout the GTT, female blood glucose levels were overall lower than male blood glucose levels ($p < 0.001$, Figure 8). Total area under the curve for female mice was also lower than male mice ($p < 0.001$, Figure 8 D), indicating that female glucose tolerance is overall higher compared to male mice.

Normalized glucose tolerance test. Although the glucose tolerance tests indicate inflammation-dependent differences in glucose metabolism, the differences in fasting blood glucose levels may amplify or distort differences in blood glucose uptake, as each curve begins at a different point along the y-axis. Therefore, we normalized blood glucose concetrations in each animal to their respective fasting blood glucose levels over the course of the GTT. This normalized value will provide a more accurate representation of the rate of glucose metabolism, as opposed to raw glucose concentrations. After normalizing to the baseline, fasting blood glucose, LPS and/or UTP treatment had no significant effect on the GTT curves or AUC (Figure 9). The AUC did however show the conserved impact of sex dependence on glucose uptake ($p < 0.001$, Figure 9 D). This data suggests that sex signigicantly afffects blood glucose during a glucose challenge. Since the observed effect of UTP and LPS in the GTT are eliminated after normalizing, this suggests that, inflammation and UTP treatment likely indirectly affect glucose tolerance through baseline glucose metabolism.

Insulin receptor and glucose transporter gene expression

To investigate the molecular determinants behind sex-dependent differences in the glucose tolerance, we quantified the gene expression of two molecules directly involved in the uptake of glucose from the blood stream: the insulin receptor and the glucose transporter

GLUT4. Following the glucose tolerance test, adipose and skeletal muscle were dissected from mice and immediately frozen in in nitrogen to prevent RNA degradation. RNA was extracted from the tissues and reverse transcribed into cDNA, which was then subject to qPCR to quantify gene expression. When comparing male and female expression, the quantification of insulin receptor in muscle ($p < 0.642$) and glucose transporter in muscle ($p < 0.214$) and adipose ($p < 0.293$) did not show any significant differences (Figure 10), suggesting that alterations in gene expression of these key regulators is not responsible for sex-dependent effects in glucose tolerance.

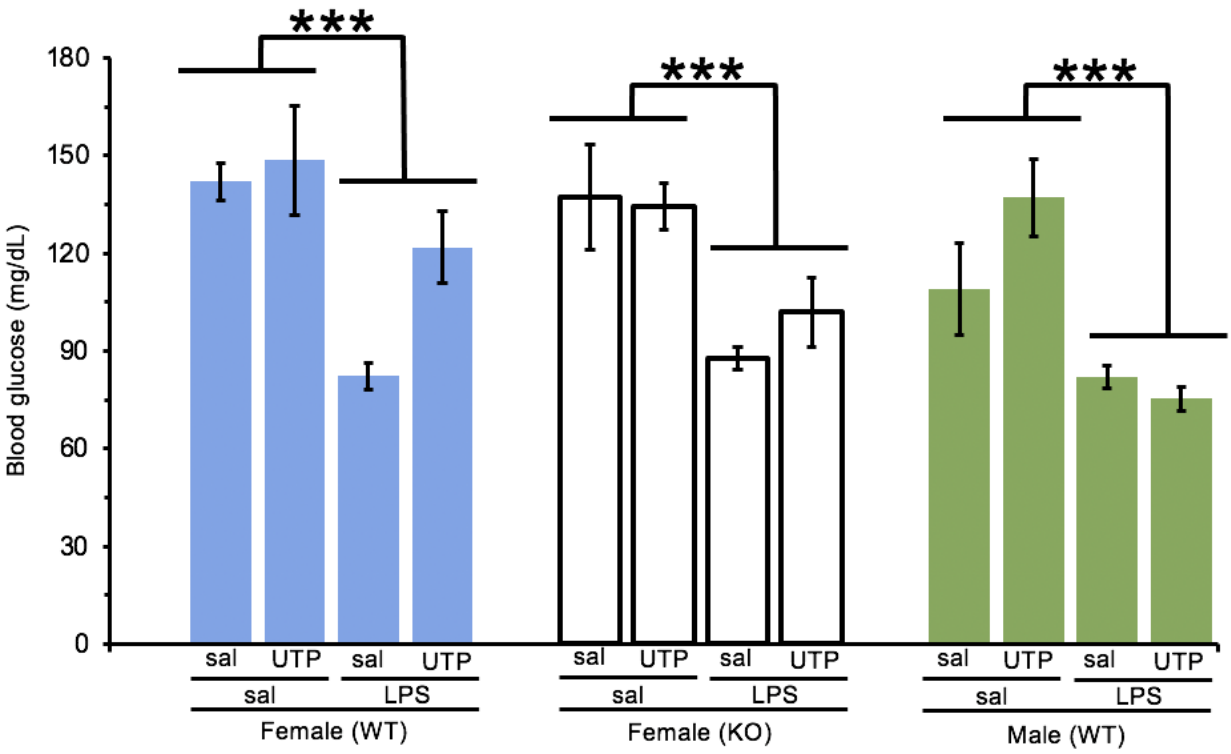

Figure 7. LPS effect on fasting blood glucose. Fasting blood glucose was measured at time 0 after a 5-hour fasting period. Female $P2Y_2R$ wildtype (WT) mice are represented as the blue filled bars (n = 22). Female $P2Y_2R$ knockout (KO) mice are represented as the black unfilled bars (n = 16). Male $P2Y_2R$ wildtype (WT) mice are represented as the green unfilled bars (n = 16). One-way ANOVA, ***$p < 0.001$, error bars = SEM

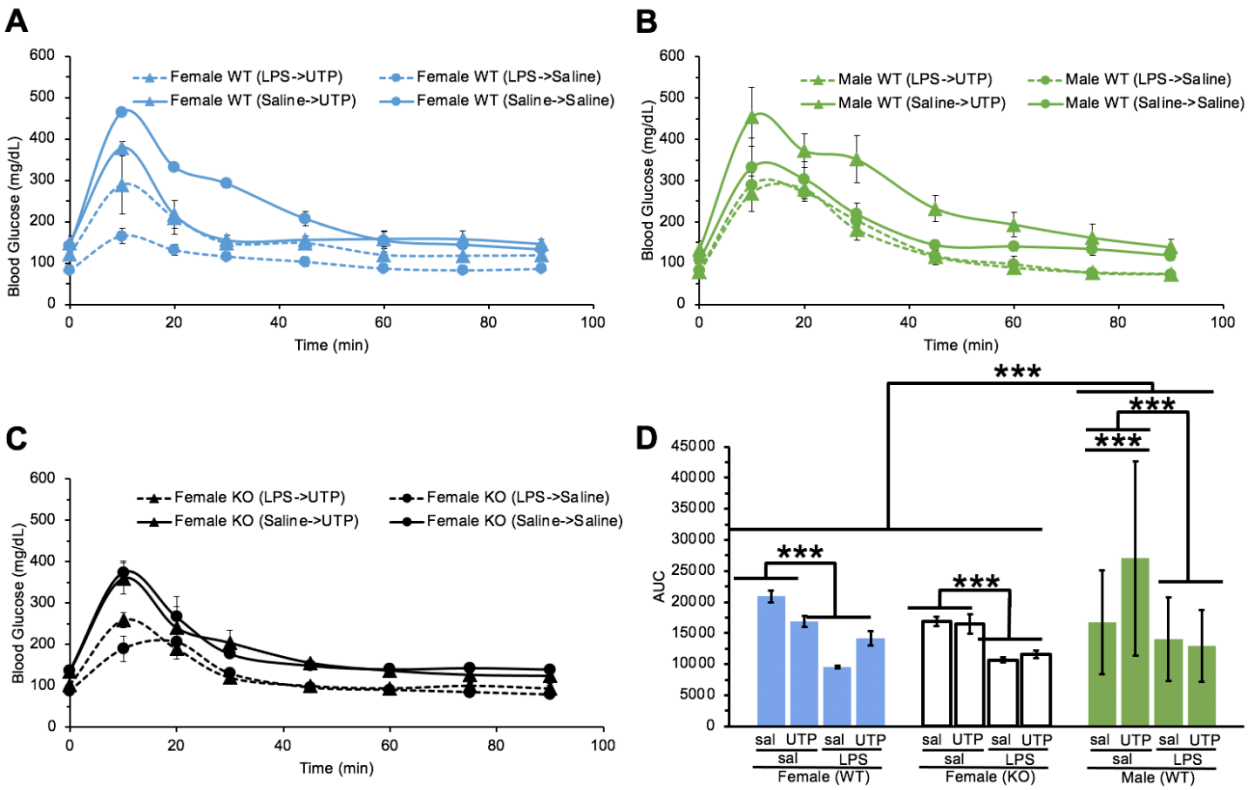

Figure 8. Raw GTT. Mice were treated with LPS (dashed line) or saline (solid line) 24 hours before the glucose tolerance test. Mice were also treated with either UTP (triangle marker) or saline (circle marker) 30 min before glucose injection. Blood glucose levels were taken at each time point over a 90-min period from (**A**) female $P2Y_2R$ wildtype (WT) mice, (**B**) male $P2Y_2R$ wildtype (WT) mice, and (**C**) female $P2Y_2R$ knockout (KO) mice. (**D**) the area under the curve (AUC) from the GTT for each group of mice. A repeated measures ANOVA (GTT) or one-way ANOVA (AUC) followed by post hoc Tukey test was performed to determine significance. ***$p < 0.001$, **$p < 0.01$, *$p < 0.05$

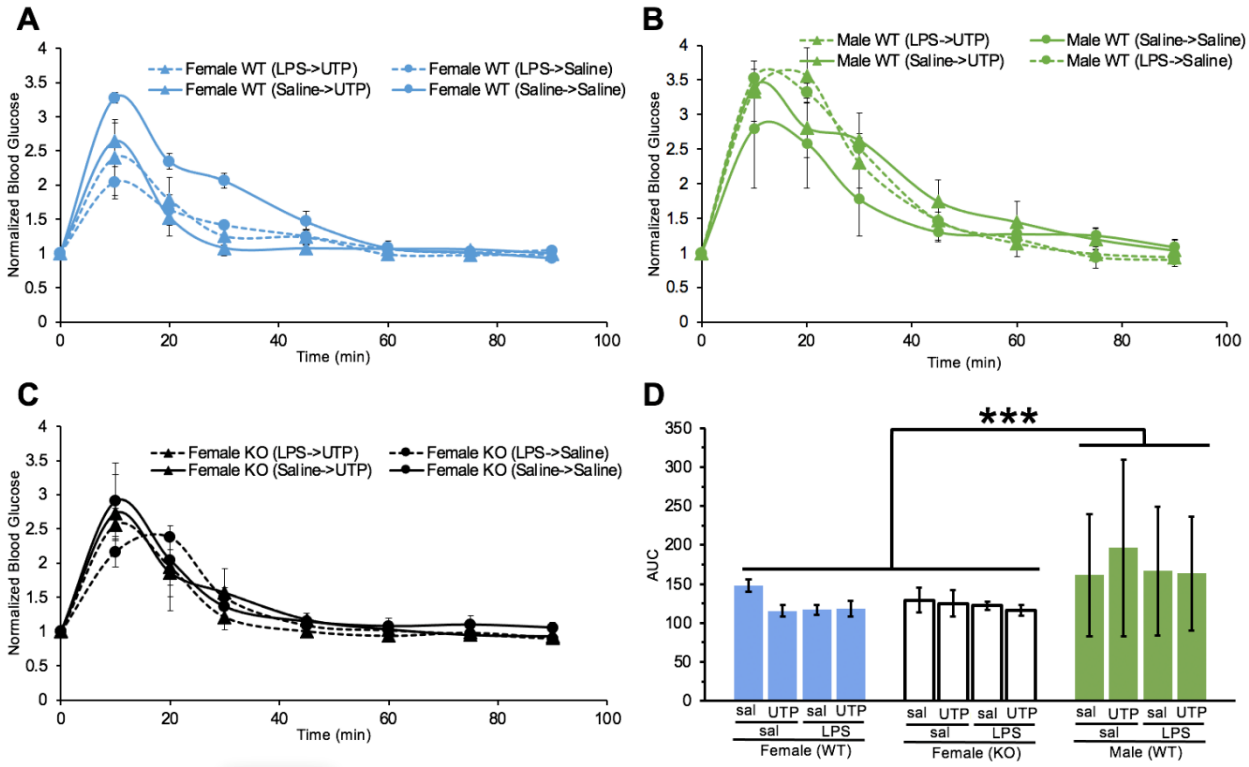

Figure 9. GTT of normalized data. Mice were treated with LPS (dashed line) or saline (solid line) 24 hours before the glucose tolerance test. Mice were also treated with either UTP (triangle marker) or saline (circle marker) 30 min before glucose injection. Raw blood glucose was normalized to the fasting blood glucose ($t = 0$) levels for each subject. The mean normalized values are shown from (**A**) female $P2Y_2R$ wildtype (WT) mice, (**B**) male $P2Y_2R$ wildtype (WT) mice, and (**C**) female $P2Y_2R$ knockout (KO) mice. (**D**) the area under the curve (AUC) for each group of mice. Repeated measures ANOVA (GTT) or one-way ANOVA (AUC) followed by post hoc Tukey test was performed to determine significance. ***$p < 0.001$

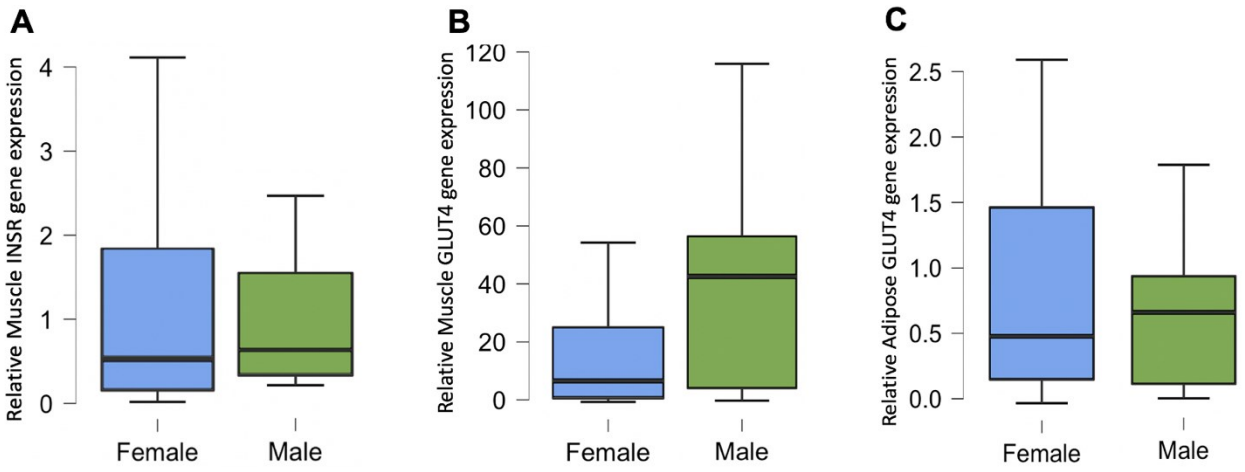

Figure 10. Effects of sex on gene expression. RNA was extracted from dissected muscle and adipose tissue of mice following glucose tolerance testing. Quantitative reverse transcription PCR was used to determine gene expression. Box and whisker plots of mean gene expression levels (+/- SEM) of glucose transporter 4 (GLUT4) measured in (**B**) muscle and (**C**) adipose, and insulin receptor (INSR) measured in (**A**) muscle only. Gene expression was compared between female (blue) and male (green) groups. A one-way ANOVA was performed.

DISCUSSION

The goal of this thesis was to investigate the effects of inflammation, $P2Y_2$ receptor activation, and sex on glucose metabolism. Overall, we found that LPS did not have an effect on glucose tolerance testing but was found to decrease fasting blood glucose levels in all mice; UTP decreased glucose tolerance in unchallenged wildtype males and did not affect females of either genotype; and female mice have an over all higher glucose tolerance than males.

The GTT curves of both female genotypes and male $P2Y_2$ wildtype mice display a similar trend. All groups reached a maximum blood glucose concentration around the 10 and 20 minute mark, followed by a steady decrease until reaching a plateau at a similar concentration to the fasting. This common trend suggests that all mice have similar rate of glucose uptake, regardless of sex or inflammatory state. However, differences in the area under these curves as well as the fasting glucose suggest that both acute inflammation and sex affect glucose homeostasis.

Fasting blood glucose regualtion

Fasting blood glucose levels are used to assess post-prandial glucose regulation. The mice in this study underwent a five hour fast to establish fasting glucose levels. Glucose concentration of mice after a 4-6 hour fast range from 80 to 100 mg/dl. However, baseline blood glucose concentrations in mice can be affected by many factors including age of the mice, conditions of fasting, and handling by researchers. The reported baseline fasting blood glucose values from various experiments exhibit considerable variability under different conditions and mouse ages. For instance, after a 4-hour fast, C57BL/6J mice at 18 weeks old show fasting blood

glucose levels ranging approximately from 138.74 to 163.96 mg/dl[84]. Male C57BL/6J mice subjected to a 12-hour daytime fast have fasting blood glucose levels ranging from about 86.0 to 106.4 mg/dl, while those from a 12-hour nighttime fast range approximately from 62.6 to 107.6 mg/dl[85]. Similarly, male C57BL/6 mice at 16 weeks old with an unspecified fasting duration showed fasting blood glucose levels ranging approximately from 117.13 to 131.53 mg/dl[86]. These results show the wide range of fasting blood glucose values influenced by fasting duration, mouse age, and specific experimental conditions.

The average fasting concentrations in this study display a larger range of 75 to 150 mg/dl (Figure 7). This variation suggests that environmental or internal factors within the study may have influenced glucose levels or the response of the mice to glucose.

The fasting blood glucose levels we collected are consistent with data from previous graduate students. In the thesis work of one previous student (Hailee Marino, 2021) compared fasting blood glucose of uninjectedmice and found that male wildtype mice had an average of 106 mg/dL, consistant with our data in which we found male wildtype mice averaged 109 mg/dL (Figure 7)[79]. However, this student also found fasting levels in unchallenged females much lower than the saline control females in our study, 88 mg/dL in female wildtype and 95 mg/dl in female knockouts, compared to our study that found 142 mg/dL in female wildtype and 137.2 mg/dL in female knockouts (Figure 7)[79].

In another student's thesis (Christian Rivas, 2023) injected both male and female mice with the same concentration of LPS, 2 mg/kg, and found similar fasting blood glucose concentration of about 80 mg/dL compared to 82 mg/dL for wildtype males, 82.25 mg/dL for wildtype females, 87.8 mg/dL for knockout females in our study (Figure 7)[81]. They also found LPS reduces fasting blood glucose in both males and females compared to the saline control

group, resulting in hypoglycemia. Inflammation induced by the treatment of mice with LPS has been shown to reduce the concentration of glucose in the blood stream by increasing insulin secretion and promoting glucose uptake[87–89].

The study environment may help explain the variation in our data and the inconcsistency with previous work. The mice in our research were seperated so male mice and female mice did not undergo experimentation in the same room to avoid the influence of mouse pheremones in our study. However, this same precaution was not take with the researchers, as the mice were handeled by a team of both male and female researchers with varying levels of training. Experimental outcomes can be influenced by the sex of their handlers. Mice exhibit more fear and stress around male handlers compared to female handlers. A study found that mice displayed reduced pain sensitivity when handled by males, likely due to heightened stress responses[90]. Further, a study investigating ketamine's effects on depression in mice revealed varying responses depending on whether the handler was male or female. Mice were injected with ketamine and their depression levels were monitored by observing swim duration. Mice swam longer when handled by male researchers, as the exposure to human male phereomones increased stress levels in mice, resulting in corticotropin-releasing factor (CRF) release. However, ketamine administered by female researchers did not trigger the release of CRF in mice [91]. Therefore, it is possible that the sex of our researchers, or the environment of our work affected the fasting glucose levels or GTT by affecting their stress levels.

LPS regulation of glucose tolerance

The treatment of LPS did not affect the glucose tolerance of wildtype males (Figure 8 B and Figure 9 B), conflicting with previous data[79]. Male wildtype mice treated with a similar dose of LPS in a similar timeline were previously shown to have a significantly decreased glucose

tolerance compare to the saline control group[79]. The discrepancy in our data collection may be attributed to the large standard deviation in glucose levels throughout GTT from male mice, potentially leading to a type I error. GTT from more male mice will reduce the likelihood of this statistical error and perhaps we would see a rejection of the null hypothesis and therefore be consistent with previous studies.

UTP-dependent effects on glucose homeostasis are insulin-independent

The P2Y family of purinergic receptors consists of eight subtypes: $P2Y_1$, $P2Y_2$, $P2Y_4$, $P2Y_6$, $P2Y_{11}$, $P2Y_{12}$, $P2Y_{13}$, and $P2Y_{14}$. UTP is known to activate four out the eight subtypes; $P2Y_2$, $P2Y_4$, $P2Y_6$, and $P2Y_{11}$[59]. $P2Y_2$ and $P2Y_6$ are the main receptor subtypes that have been implicated in disruption of glucose metabolism[61,92]. Therefore, to determine if the effects we see from UTP administration are from the $P2Y_2$ receptor, we must compare the results obtained from UTP treated wildtype animals to the $P2Y_2$ receptor knockout model. If the GTT results of $P2Y_2$ knockout male mice mirror the results from the wildtype mice, the effects we see may be from another P2Y receptor.

$P2Y_2$ and $P2Y_6$ are the main receptor subtypes that have been implicated in disruption of glucose metabolism. Therefore, to determine if the effects we see from UTP administration are from the $P2Y_2$ receptor, we must compare the results obtained from UTP treated wildtype animals to the $P2Y_2$ receptor knockout model. If the results between genotypes are insignificant, we can conclude that the $P2Y_2$ receptor is not responsible.

The only affect of UTP was seen in the raw glucose tolerance data in male wildtype animals (Figure 8 B). Due to limited availability of male $P2Y_2$ knockout mice, we are unable to determine if the effect of UTP is due to stimulation of the $P2Y_2$ receptor or through another mechanism, such as stimulation of $P2Y_6$R. In the future, the completion of GTT in $P2Y_2$R

knockout animals treated with UTP will provide additional insights into the effect of $P2Y_2R$ in glucose tolerance. It is important that these future glucose tolerance tests be well controlled, with a similar team of researchers performing GTT for both wildtype and knockout animals in a similar time frame.

Glucose tolerance in female mice was not affected by UTP treatment. We also did not observe any significant differences of glucose tolerance in $P2Y_2$ knockout females compared to wildtype females (Figure 8 A, C, D and Figure 9 A, C, D). This is consistent with previous research[79] and supports the finding that glucose metabolism in female mice is not regulated by the $P2Y_2$ receptor. Because $P2Y_2$ has not been shown to regulate glucose metabolism in females, UTP was not expected to affect the GTT.

In the presence of inflammation, $P2Y_2$ receptor knockout male mice were previously shown to have increased glucose tolerance compared to wildtype male mice, suggesting that $P2Y_2R$ decreases glucose uptake during acute inflammation in males[79]. Therefore, UTP stimulation of the $P2Y_2$ receptor in wildtype male mice was anticipated to decrease glucose tolerance compared to the saline control. We found that UTP decreased glucose tolerance in male mice, but not during LPS-induced inflammation or after normalizing (Figure 8 B, D and Figure 9 B, D), suggesting that primary effects of $P2Y_2R$ are during baseline, unchallenged conditions and therefore are insulin-independent. Further study into the effect of UTP on insulin-dependence can be tested with an insulin tolerance test or an insulin enzyme linked immunosorbent assay (ELISA). If UTP induced $P2Y_2R$ effects are insulin independent, we would not expect to see differences in blood glucose levels after the injection of insulin, or in the levels of plasma insulin in UTP treated mice.

While UTP had a small effect on blood glucose during GTT in male wildtype mice, this affect is eliminated in GTT after normalizing blood glucose levels to fasting. It is possible that the small observed affect is due to a type II error that can be corrected by increasing our sample number. Regardless, the lack of affect in the normalized data may be because the concentration of UTP used was not high enough and/or it could have degraded post-injection. UTP is an ribonucleotide with a high oxygen content, and therefore high potential for nucleophilic attack. The injected UTP might have been degraded by RNases or autohydrolysis before its effects could be recorded. Continuous perfusion of UTP during GTT may replenish UTP to assure intact UTP is avaiable to cells and tissues. Alternatively, a higher single-dose UTP concentration may be more effective. Studies utilizing an IP injection of UTP in mice are limited. It may be necessary to find a more optimal UTP concentration for *in vivo* $P2Y_2$ stimulation by injecting mice with increasing concentrations of UTP and determining if these higher doses affect GTT.

Sex-dependent effects on glucose metabolism

Literature on sex specific variences in glucose tolerance in $P2Y_2$ receptor knockout animals is very limited. Our results show that female $P2Y_2R$ knockout mice also displayed insignificant differences in blood glucose levels across the GTT compared to female wildtype mice (Figure 8 D and Figure 9 D), however we did not have male $P2Y_2$ knockout mice for comparison. During the glucose tolerance test, comparing the area under the curve shows rate of glucose accumulation and clearance was lower in male mice compared to female mice, but the fasting glucose levels were similar between sexes. This suggests differences in metabolic characteristics between sexes are insulin dependent. Previous literature also shows that female mice have lower blood glucose levels during glucose tolerance tests and higher glucose tolerance

than male mice. This supports the findings that sex hormones such as estrogen enhance insulin sensitivity[93], suggesting this sex-dependent phenomenon may also be true in humans.

The inflammatory status of the mice did not result in significant effects on the glucose tolerance of either sex. LPS treatment lowered blood glucose concentrations throughout the entire GTT and in the fasting state (Figure 8 and Figure 7, respectively). However, because the fasting blood glucose levels of LPS-treated mice were significantly lower than than the saline control, the GTT curves were normalized to evaluate the influence and rate of glucose uptake. The normalized curves (Figure 9 A-B) show that LPS-induced inflammation did not affect glucose tolerance in male or female mice. Previous studies have shown that inflammation in male wildtype mice resulted in a decrease in glucose tolerance compared to a saline control, however, this affect was lacking in female mice[61,79,94]. We are confident in the environment and methods used to collect GTT data from female mice, which is reflected in the low variance at each data point. This data is also consistent with previous research. However, when testing occurred on male mice, additional researchers with less experience joined the research team. To accommodate these individuals, the time of day and location of the tests were varied. These additional variables may have increased the variability of the data, decreasing statistical power. It is necessary to increase the number of male animals to ensure confidence in the data. Perhaps, with increased power, the data may agree with previous studies.

Sex-dependent gene expression. To explain the sex-dependent differences in glucose tolerance, we quantified gene expression of the insulin receptor (INSR) in skeletal muscle and glucose transporter 4 (GLUT4) in skeletal muscle and adipose tissue of the mice we subjected to GTT. Skeletal muscle and adipose tissue are two major metabolic tissues and are responsible for

over 90% of glucose uptake and storage. Glucose uptake into the cell occurs across GLUT4 and the opening of this transporter is dependent on insulin receptor activation.

Because glucose tolerance was found to be higher in females than in males, we anticipated that GLUT4 and INSR expression would be increased in females. Previous research has shown that insulin receptor expression in skeletal muscle is increased in females[95], therefore we expected a similar result. However, we did not observe any significant differences between expression of INSR or GLUT4 in male or female skeletal muscle and adipose tissue (Figure 10 A-C), suggesting that differences in gene expression do not account for sex-differences. It may be that sex-specific changes in blood glucose concentrations are not influenced by mRNA levels but may be dependent on insulin signaling in adipose and muscle tissue.

Insulin binding to the insulin receptor causes the translocation of GLUT4 containing vesicle to deposit glucose transporters on the membrane. Therefore, the distribution of GLUT4 may be affected by sex, without affecting the overall expression of GLUT4. In this case, it is possible that female mice may have more GLUT4 transporters deposited on the surface cell membranes, while GLUT4 is distributed more internally in male mice. We can test this aspect of our experiment by measuring the amount of GLUT4 expressed on the membrane of the tissues with microscopy, cell fractionation, or flowcytometry. We would expect that female mice have an increased GLUT4 on the membrane surface compared to male mice. Our data is also limited to gene expression of adipose and skeletal muscle and does not eliminate the potential for sex-dependent gene expression changes in other cell types. Due to limited mouse availability, the data collected is preliminary and more research is needed to draw further conclusions.

Implications

Our research has the potential to enhance understanding of how acute inflammation affects glucose metabolism in males and females. Treatments for disruptions in glucose metabolism are currently the same for both men and women, however our data shows marked sex-based variations in the physiology of glucose metabolism. For example, Metformin is the most common drug prescribed to patients with type 2 diabetes, however the mechanism of action was not known until recently. A 2023 study shows that metformin treats insulin resistance by attenuating activation of the $P2Y_2$ receptor[96]. If $P2Y_2$ receptor-dependent effects are on glucose metabolism are male-specific, then the most prescribed treatment for the fastest growing chronic disease in the United States may be effective for only males. Inclusive research that takes aim at understanding these sex-dependence could yield new directions for developing specialized pharmaceutical targeting that optimizes therapeutic potential.

REFERENCES

1. Röder, P.V., Wu, B., Liu, Y., and Han, W. (2016). Pancreatic regulation of glucose homeostasis. Exp. Mol. Med. *48*, e219.

2. Boucher, J., Kleinridders, A., and Kahn, C.R. (2014). Insulin receptor signaling in normal and insulin-resistant states. Cold Spring Harb. Perspect. Biol. *6*. 10.1101/cshperspect.a009191.

3. De Meyts, P. (2016). The Insulin Receptor and Its Signal Transduction Network. In Endotext, K. R. Feingold, B. Anawalt, M. R. Blackman, A. Boyce, G. Chrousos, E. Corpas, W. W. de Herder, K. Dhatariya, K. Dungan, J. Hofland, et al., eds. (MDText.com, Inc.).

4. Beaulieu, J.-M. (2012). A role for Akt and glycogen synthase kinase-3 as integrators of dopamine and serotonin neurotransmission in mental health. J. Psychiatry Neurosci. *37*, 7–16.

5. Beurel, E., Grieco, S.F., and Jope, R.S. (2015). Glycogen synthase kinase-3 (GSK3): regulation, actions, and diseases. Pharmacol. Ther. *148*, 114–131.

6. Navale, A.M., and Paranjape, A.N. (2016). Glucose transporters: physiological and pathological roles. Biophys. Rev. *8*, 5–9.

7. Thorens, B., and Mueckler, M. (2010). Glucose transporters in the 21st Century. Am. J. Physiol. Endocrinol. Metab. *298*, E141-5.

8. Thorens, B. (2015). GLUT2, glucose sensing and glucose homeostasis. Diabetologia *58*, 221–232.

9. Huang, S., and Czech, M.P. (2007). The GLUT4 glucose transporter. Cell Metab. *5*, 237–252.

10. Stanfield, C.L. (2018). Principles of Human Physiology, 6th edition Sixth. (Pearson Education).

11. Merz, K.E., and Thurmond, D.C. (2020). Role of Skeletal Muscle in Insulin Resistance and Glucose Uptake. Compr. Physiol. *10*, 785–809.

12. Wasserman, D.H., Kang, L., Ayala, J.E., Fueger, P.T., and Lee-Young, R.S. (2011). The physiological regulation of glucose flux into muscle in vivo. J. Exp. Biol. *214*, 254–262.

13. Meyer, C., Dostou, J.M., Welle, S.L., and Gerich, J.E. (2002). Role of human liver, kidney, and skeletal muscle in postprandial glucose homeostasis. Am. J. Physiol. Endocrinol. Metab. *282*, E419-27.

14. Cypess, A.M., Lehman, S., Williams, G., Tal, I., Rodman, D., Goldfine, A.B., Kuo, F.C., Palmer, E.L., Tseng, Y.-H., Doria, A., et al. (2009). Identification and importance of brown adipose tissue in adult humans. N. Engl. J. Med. *360*, 1509–1517.

15. Kimura, T., Pydi, S.P., Wang, L., Haspula, D., Cui, Y., Lu, H., König, G.M., Kostenis, E., Steinberg, G.R., Gavrilova, O., et al. (2022). Adipocyte Gq signaling is a regulator of glucose and lipid homeostasis in mice. Nat. Commun. *13*, 1652.

16. Lee, S.-H., Park, S.-Y., and Choi, C.S. (2022). Insulin Resistance: From Mechanisms to Therapeutic Strategies. Diabetes Metab. J. *46*, 15–37.

17. Galicia-Garcia, U., Benito-Vicente, A., Jebari, S., Larrea-Sebal, A., Siddiqi, H., Uribe, K.B., Ostolaza, H., and Martín, C. (2020). Pathophysiology of Type 2 Diabetes Mellitus. Int. J. Mol. Sci. *21*. 10.3390/ijms21176275.

18. Welz, B., Bikker, R., Hoffmeister, L., Diekmann, M., Christmann, M., Brand, K., and Huber, R. (2021). Activation of GSK3 Prevents Termination of TNF-Induced Signaling. J. Inflamm. Res. *14*, 1717–1730.

19. National Diabetes Statistics Report (2023). https://www.cdc.gov/diabetes/data/statistics-report/index.html.

20. Lucier, J., and Weinstock, R.S. (2023). Type 1 Diabetes (StatPearls Publishing).

21. Giwa, A.M., Ahmed, R., Omidian, Z., Majety, N., Karakus, K.E., Omer, S.M., Donner, T., and Hamad, A.R.A. (2020). Current understandings of the pathogenesis of type 1 diabetes: Genetics to environment. World J. Diabetes *11*, 13–25.

22. Reed, J., Bain, S., and Kanamarlapudi, V. (2021). A Review of Current Trends with Type 2 Diabetes Epidemiology, Aetiology, Pathogenesis, Treatments and Future Perspectives. Diabetes Metab. Syndr. Obes. *14*, 3567–3602.

23. Rask-Madsen, C., and King, G.L. (2013). Vascular complications of diabetes: mechanisms of injury and protective factors. Cell Metab. *17*, 20–33.

24. Kadl, A., and Leitinger, N. (2005). The role of endothelial cells in the resolution of acute inflammation. Antioxid. Redox Signal. *7*, 1744–1754.

25. Diabetes (2024). https://www.mayoclinic.org/diseases-conditions/diabetes/diagnosis-treatment/drc-20371451.

26. Burnstock, G., and Novak, I. (2013). Purinergic signalling and diabetes. Purinergic Signal. *9*, 307–324.

27. Khin, P.P., Lee, J.H., and Jun, H.-S. (2023). Pancreatic Beta-cell Dysfunction in Type 2 Diabetes. Eur. J. Inflam. *21*, 1721727X231154152.

28. Rhea, E.M., Banks, W.A., and Raber, J. (2022). Insulin Resistance in Peripheral Tissues and the Brain: A Tale of Two Sites. Biomedicines *10*. 10.3390/biomedicines10071582.

29. Khalid, M., Alkaabi, J., Khan, M.A.B., and Adem, A. (2021). Insulin Signal Transduction Perturbations in Insulin Resistance. Int. J. Mol. Sci. *22*. 10.3390/ijms22168590.

30. Donath, M.Y., and Shoelson, S.E. (2011). Type 2 diabetes as an inflammatory disease. Nat. Rev. Immunol. *11*, 98–107.

31. Butler, S.O., Btaiche, I.F., and Alaniz, C. (2005). Relationship between hyperglycemia and infection in critically ill patients. Pharmacotherapy *25*, 963–976.

32. Shi, J., Fan, J., Su, Q., and Yang, Z. (2019). Cytokines and Abnormal Glucose and Lipid Metabolism. Front. Endocrinol. *10*, 703.

33. Mignemi, N.A., McClatchey, P.M., Kilchrist, K.V., Williams, I.M., Millis, B.A., Syring, K.E., Duvall, C.L., Wasserman, D.H., and McGuinness, O.P. (2019). Rapid changes in the microvascular circulation of skeletal muscle impair insulin delivery during sepsis. Am. J. Physiol. Endocrinol. Metab. *316*, E1012–E1023.

34. Pal, S., Nath, P., Das, D., Hajra, S., and Maitra, S. (2018). Cross-talk between insulin signalling and LPS responses in mouse macrophages. Mol. Cell. Endocrinol. *476*, 57–69.

35. House, L.M., 2nd, Morris, R.T., Barnes, T.M., Lantier, L., Cyphert, T.J., McGuinness, O.P., and Otero, Y.F. (2015). Tissue inflammation and nitric oxide-mediated alterations in cardiovascular function are major determinants of endotoxin-induced insulin resistance. Cardiovasc. Diabetol. *14*, 56.

36. Gyawali, B., Ramakrishna, K., and Dhamoon, A.S. (2019). Sepsis: The evolution in definition, pathophysiology, and management. SAGE Open Med *7*, 2050312119835043.

37. Pålsson-McDermott, E.M., and O'Neill, L.A.J. (2004). Signal transduction by the lipopolysaccharide receptor, Toll-like receptor-4. Immunology *113*, 153–162.

38. Mendes de Oliveira, E., Silva, J.C., Ascar, T.P., Sandri, S., Marchi, A.F., Migliorini, S., Nakaya, H.T.I., Fock, R.A., and Campa, A. (2022). Acute Inflammation Is a Predisposing Factor for Weight Gain and Insulin Resistance. Pharmaceutics *14*. 10.3390/pharmaceutics14030623.

39. Giugliano, D., Ceriello, A., and Esposito, K. (2008). Glucose metabolism and hyperglycemia. Am. J. Clin. Nutr. *87*, 217S-222S.

40. Wellen, K.E., and Hotamisligil, G.S. (2005). Inflammation, stress, and diabetes. J. Clin. Invest. *115*, 1111–1119.

41. Han, H.-S., Kang, G., Kim, J.S., Choi, B.H., and Koo, S.-H. (2016). Regulation of glucose metabolism from a liver-centric perspective. Exp. Mol. Med. *48*, e218–e218.

42. Plomgaard, P., Bouzakri, K., Krogh-Madsen, R., Mittendorfer, B., Zierath, J.R., and Pedersen, B.K. (2005). Tumor necrosis factor-alpha induces skeletal muscle insulin resistance in healthy human subjects via inhibition of Akt substrate 160 phosphorylation. Diabetes *54*, 2939–2945.

43. Hotamisligil, G.S., Murray, D.L., Choy, L.N., and Spiegelman, B.M. (1994). Tumor necrosis factor alpha inhibits signaling from the insulin receptor. Proc. Natl. Acad. Sci. U. S. A. *91*, 4854–4858.

44. Feng, W., Liu, Y., Fei, F., Chen, Y., Ding, Y., Yan, M., Feng, Y., Zhao, T., Mao, G., Yang, L., et al. (2018). Improvement of high-glucose and insulin resistance of chromium malate in 3T3-L1 adipocytes by glucose uptake and insulin sensitivity signaling pathways and its mechanism. RSC Adv. *9*, 114–127.

45. Hotamisligil, G.S., Arner, P., Caro, J.F., Atkinson, R.L., and Spiegelman, B.M. (1995). Increased adipose tissue expression of tumor necrosis factor-alpha in human obesity and insulin resistance. J. Clin. Invest. *95*, 2409–2415.

46. Cawthorn, W.P., and Sethi, J.K. (2008). TNF-alpha and adipocyte biology. FEBS Lett. *582*, 117–131.

47. Sarikaya, E. (2018). Functions of Purinergic Receptors. Receptors P1 and P2 as Targets for Drug Therapy in Humans.

48. Jacobson, K.A., Balasubramanian, R., Deflorian, F., and Gao, Z.-G. (2012). G protein-coupled adenosine (P1) and P2Y receptors: ligand design and receptor interactions. Purinergic Signal. *8*, 419–436.

49. Jacobson, K.A., Costanzi, S., Joshi, B.V., Besada, P., Shin, D.H., Ko, H., Ivanov, A.A., and Mamedova, L. (2006). Agonists and antagonists for P2 receptors. Novartis Found. Symp. *276*, 58–68; discussion 68-72, 107–112, 275–281.

50. Choi, R.C.Y., Chu, G.K.Y., Siow, N.L., Yung, A.W.Y., Yung, L.Y., Lee, P.S.C., Lo, C.C.W., Simon, J., Dong, T.T.X., Barnard, E.A., et al. (2013). Activation of UTP-sensitive P2Y2 receptor induces the expression of cholinergic genes in cultured cortical neurons: a signaling cascade triggered by Ca2+ mobilization and extracellular regulated kinase phosphorylation. Mol. Pharmacol. *84*, 50–61.

51. Nasrullah, M.Z., Peng, Q., and Shen, J. (2019). The P2Y2 receptor mediates hyperglycemia-induced insulin resistance in human skeletal muscle cells. FASEB J. *33*. 10.1096/fasebj.2019.33.1_supplement.514.3.

52. Merz, J., Albrecht, P., von Garlen, S., Ahmed, I., Dimanski, D., Wolf, D., Hilgendorf, I., Härdtner, C., Grotius, K., Willecke, F., et al. (2018). Purinergic receptor Y2 (P2Y2)-dependent VCAM-1 expression promotes immune cell infiltration in metabolic syndrome. Basic Res. Cardiol. *113*, 45.

53. Woo, S.-H., and Trinh, T.N. (2020). P2 Receptors in Cardiac Myocyte Pathophysiology and Mechanotransduction. Int. J. Mol. Sci. *22*. 10.3390/ijms22010251.

54. Vallon, V., Stockand, J., and Rieg, T. (2012). P2Y receptors and kidney function. Wiley Interdiscip. Rev. Membr. Transp. Signal. *1*, 731–742.

55. Homolya, L., Watt, W.C., Lazarowski, E.R., Koller, B.H., and Boucher, R.C. (1999). Nucleotide-regulated Calcium Signaling in Lung Fibroblasts and Epithelial Cells from Normal and P2Y2 Receptor (−/−) Mice *. J. Biol. Chem. *274*, 26454–26460.

56. Sojka, A.C., Brennan, K.M., Maizels, E.T., and Young, C.D. (2017). The Science Behind G Protein-Coupled Receptors (GPCRs) and Their Accurate Visual Representation in Scientific Research. J. Biocommun. *41*, e6.

57. Liu, J., Liao, Z., Camden, J., Griffin, K.D., Garrad, R.C., Santiago-Pérez, L.I., González, F.A., Seye, C.I., Weisman, G.A., and Erb, L. (2004). Src homology 3 binding sites in the P2Y2 nucleotide receptor interact with Src and regulate activities of Src, proline-rich tyrosine kinase 2, and growth factor receptors. J. Biol. Chem. *279*, 8212–8218.

58. Zhang, L., and Shi, G. (2016). Gq-Coupled Receptors in Autoimmunity. J Immunol Res *2016*, 3969023.

59. Erb, L., and Weisman, G.A. (2012). Coupling of P2Y receptors to G proteins and other signaling pathways. Wiley Interdiscip. Rev. Membr. Transp. Signal. *1*, 789–803.

60. Song, Z., Wang, Y., Zhang, F., Yao, F., and Sun, C. (2019). Calcium Signaling Pathways: Key Pathways in the Regulation of Obesity. Int. J. Mol. Sci. *20*. 10.3390/ijms20112768.

61. Zhang, Y., Ecelbarger, C.M., Lesniewski, L.A., Müller, C.E., and Kishore, B.K. (2020). P2Y2 Receptor Promotes High-Fat Diet-Induced Obesity. Front. Endocrinol. *11*, 341.

62. Senfeld, J.I., and Shen, J. (2020). Evidence for P2Y2 receptor facilitation of hyperglycemia-induced insulin resistance in human hepatocytes. FASEB J. *34*, 1–1.

63. Ciarambino, T., Crispino, P., Guarisco, G., and Giordano, M. (2023). Gender Differences in Insulin Resistance: New Knowledge and Perspectives. Curr. Issues Mol. Biol. *45*, 7845–7861.

64. Mauvais-Jarvis, F., Clegg, D.J., and Hevener, A.L. (2013). The role of estrogens in control of energy balance and glucose homeostasis. Endocr. Rev. *34*, 309–338.

65. Mauvais-Jarvis, F. (2018). Gender differences in glucose homeostasis and diabetes. Physiol. Behav. *187*, 20–23.

66. Macotela, Y., Boucher, J., Tran, T.T., and Kahn, C.R. (2009). Sex and depot differences in adipocyte insulin sensitivity and glucose metabolism. Diabetes *58*, 803–812.

67. Yi, P., Wang, Z., Feng, Q., Chou, C.-K., Pintilie, G.D., Shen, H., Foulds, C.E., Fan, G., Serysheva, I., Ludtke, S.J., et al. (2017). Structural and Functional Impacts of ER Coactivator Sequential Recruitment. Mol. Cell *67*, 733-743.e4.

68. Arcones, A.C., Cruces-Sande, M., Ramos, P., Mayor, F., Jr, and Murga, C. (2019). Sex Differences in High Fat Diet-Induced Metabolic Alterations Correlate with Changes in the Modulation of GRK2 Levels. Cells *8*. 10.3390/cells8111464.

69. Chamekh, M., and Casimir, G. (2019). Editorial: Sexual Dimorphism of the Immune Inflammatory Response in Infectious and Non-infectious Diseases. Front. Immunol. *10*, 107.

70. Asai, K., Hiki, N., Mimura, Y., Ogawa, T., Unou, K., and Kaminishi, M. (2001). Gender differences in cytokine secretion by human peripheral blood mononuclear cells: role of estrogen in modulating LPS-induced cytokine secretion in an ex vivo septic model. Shock *16*, 340–343.

71. Harding, A.T., and Heaton, N.S. (2022). The Impact of Estrogens and Their Receptors on Immunity and Inflammation during Infection. Cancers *14*. 10.3390/cancers14040909.

72. Slavich, G.M., and Sacher, J. (2019). Stress, sex hormones, inflammation, and major depressive disorder: Extending Social Signal Transduction Theory of Depression to account for sex differences in mood disorders. Psychopharmacology *236*, 3063–3079.

73. Pisitkun, P., Deane, J.A., Difilippantonio, M.J., Tarasenko, T., Satterthwaite, A.B., and Bolland, S. (2006). Autoreactive B cell responses to RNA-related antigens due to TLR7 gene duplication. Science *312*, 1669–1672.

74. Tang, D., Kang, R., Coyne, C.B., Zeh, H.J., and Lotze, M.T. (2012). PAMPs and DAMPs: signal 0s that spur autophagy and immunity. Immunol. Rev. *249*, 158–175.

75. Brown, G.J., Cañete, P.F., Wang, H., Medhavy, A., Bones, J., Roco, J.A., He, Y., Qin, Y., Cappello, J., Ellyard, J.I., et al. (2022). TLR7 gain-of-function genetic variation causes human lupus. Nature *605*, 349–356.

76. Mishra, H., Schlack-Leigers, C., Lim, E.L., Thieck, O., Magg, T., Raedler, J., Wolf, C., Klein, C., Ewers, H., Lee-Kirsch, M.A., et al. (2024). Disrupted degradative sorting of TLR7 is associated with human lupus. Science Immunology *9*, eadi9575.

77. Chlamydas, S., Markouli, M., Strepkos, D., and Piperi, C. (2022). Epigenetic mechanisms regulate sex-specific bias in disease manifestations. J. Mol. Med. *100*, 1111–1123.

78. Rettew, J.A., Huet-Hudson, Y.M., and Marriott, I. (2008). Testosterone reduces macrophage expression in the mouse of toll-like receptor 4, a trigger for inflammation and innate immunity. Biol. Reprod. *78*, 432–437.

79. Ulbricht, R.J., Rivas, C.A., Marino, H., Snyder, E., James, D., Makhloufi, J., Johnson, N., Zimmerman, S., and Wang, J. (2023). Sex-specific effect of P2Y2 purinergic receptor on glucose metabolism during acute inflammation. Front. Endocrinol. *14*, 1248139.

80. Pfaffl, M.W. (2001). A new mathematical model for relative quantification in real-time RT-PCR. Nucleic Acids Res. *29*, e45.

81. Rivas, C.A. SSex-dependent ESSex-dependent effects of induced acute inflammation on ffects of induced acute inflammation on glucose homeostasis and RNGlucose homeostasis and RNA editing enzymes A editing enzymes. https://bearworks.missouristate.edu/cgi/viewcontent.cgi?article=4940&context=theses.

82. Yea, K., Kim, J., Lim, S., Kwon, T., Park, H.S., Park, K.S., Suh, P.-G., and Ryu, S.H. (2009). Lysophosphatidylserine regulates blood glucose by enhancing glucose transport in myotubes and adipocytes. Biochem. Biophys. Res. Commun. *378*, 783–788.

83. Schuster, D.P., Brody, S.L., Zhou, Z., Bernstein, M., Arch, R., Link, D., and Mueckler, M. (2007). Regulation of lipopolysaccharide-induced increases in neutrophil glucose uptake. Am. J. Physiol. Lung Cell. Mol. Physiol. *292*, L845-51.

84. Hull, R.L., Willard, J.R., Struck, M.D., Barrow, B.M., Brar, G.S., Andrikopoulos, S., and Zraika, S. (2017). High fat feeding unmasks variable insulin responses in male C57BL/6 mouse substrains. J. Endocrinol. *233*, 53–64.

85. Sun, C., Li, X., Liu, L., Canet, M., Guan, Y., Fan, Y., and Zhou, Y. (2016). Effect of fasting time on measuring mouse blood glucose level. https://www.semanticscholar.org › paper › Effect-of-fas...https://www.semanticscholar.org › paper › Effect-of-fas...

86. Funkat, A., Massa, C.M., Jovanovska, V., Proietto, J., and Andrikopoulos, S. (2004). Metabolic adaptations of three inbred strains of mice (C57BL/6, DBA/2, and 129T2) in response to a high-fat diet. J. Nutr. *134*, 3264–3269.

87. Mészáros, K., Lang, C.H., Bagby, G.J., and Spitzer, J.J. (1987). Contribution of different organs to increased glucose consumption after endotoxin administration. J. Biol. Chem. *262*, 10965–10970.

88. Lang, C.H. (1995). Neural regulation of the enhanced uptake of glucose in skeletal muscle after endotoxin. Am. J. Physiol. *269*, R437-44.

89. Dridi, L., Seyrantepe, V., Fougerat, A., Pan, X., Bonneil, E., Thibault, P., Moreau, A., Mitchell, G.A., Heveker, N., Cairo, C.W., et al. (2013). Positive regulation of insulin signaling by neuraminidase 1. Diabetes *62*, 2338–2346.

90. Katsnelson, A. (2014). Male researchers stress out rodents. Nature Publishing Group UK. 10.1038/nature.2014.15106.

91. Georgiou, P., Zanos, P., Mou, T.-C.M., An, X., Gerhard, D.M., Dryanovski, D.I., Potter, L.E., Highland, J.N., Jenne, C.E., Stewart, B.W., et al. (2022). Experimenters' sex

modulates mouse behaviors and neural responses to ketamine via corticotropin releasing factor. Nat. Neurosci. *25*, 1191–1200.

92. Balasubramanian, R., Robaye, B., Boeynaems, J.-M., and Jacobson, K.A. (2014). Enhancement of glucose uptake in mouse skeletal muscle cells and adipocytes by P2Y6 receptor agonists. PLoS One *9*, e116203.

93. Yan, H., Yang, W., Zhou, F., Li, X., Pan, Q., Shen, Z., Han, G., Newell-Fugate, A., Tian, Y., Majeti, R., et al. (2019). Estrogen Improves Insulin Sensitivity and Suppresses Gluconeogenesis via the Transcription Factor Foxo1. Diabetes *68*, 291–304.

94. Wu, Y., Wu, T., Wu, J., Zhao, L., Li, Q., Varghese, Z., Moorhead, J.F., Powis, S.H., Chen, Y., and Ruan, X.Z. (2013). Chronic inflammation exacerbates glucose metabolism disorders in C57BL/6J mice fed with high-fat diet. J. Endocrinol. *219*, 195–204.

95. Lundsgaard, A.-M., and Kiens, B. (2014). Gender differences in skeletal muscle substrate metabolism - molecular mechanisms and insulin sensitivity. Front. Endocrinol. *5*, 195.

96. Senfeld, J., Peng, Q., Shi, Y., Qian, S., and Shen, J. (2023). A purinergic mechanism underlying metformin regulation of hyperglycemia. iScience *26*, 106898.

APPENDICES

Appendix A. CITI training certificate.

CITI PROGRAM

Completion Date 21-Feb-2023
Expiration Date N/A
Record ID 54422900

This is to certify that:

Jamila Makhloufi

Not valid for renewal of certification through CME.

Has completed the following CITI Program course:

Working with Mice in Research Settings
(Curriculum Group)
Working with Mice
(Course Learner Group)
1 - Basic Course
(Stage)

Under requirements set by:

Missouri State University

CITI
Collaborative Institutional Training Initiative

101 NE 3rd Avenue, Suite 120
Fort Lauderdale, FL 33301 US
www.citiprogram.org

Verify at www.citiprogram.org/verify/?w046b2785-5c6f-40d8-af24-e3fd36b874d2-54422900

CITI PROGRAM

Completion Date 22-Feb-2023
Expiration Date N/A
Record ID 54422899

This is to certify that:

Jamila Makhloufi

Not valid for renewal of certification through CME.

Has completed the following CITI Program course:

Reducing Pain and Distress in Laboratory Mice and Rats
(Curriculum Group)
Reducing Pain and Distress in Laboratory Mice and Rats
(Course Learner Group)
1 - Basic Course
(Stage)

Under requirements set by:

Missouri State University

CITI
Collaborative Institutional Training Initiative

101 NE 3rd Avenue, Suite 120
Fort Lauderdale, FL 33301 US
www.citiprogram.org

Verify at www.citiprogram.org/verify/?w2e18c1dc-4c13-4155-8d4d-6ce50eb82717-54422899

Appendix B. IACUC protocol approval

Missouri State
UNIVERSITY

September 27, 2023

RE: IACUC protocol 2021-02

Jamila Makhloufi,

IACUC protocol # 2021-02 entitled "Glucose Tolerance Test in the P2Y2 Knockout mouse" was approved by the committee on February 5, 2021 expiring February 4, 2025.

The protocol reflects that you were approved to work with Dr. Jianjie Wang and Dr. Randi Ulbricht on this project.

Thank you and if you need anything in the future regarding these protocols, please contact me either via email (johnnapedersen@missouristate.edu) or at 417-836-3737.

Sincerely,

Johnna Pedersen

Johnna Pedersen
IACUC Administrator/Member
Interim Director of Research Administration

OFFICEOFRESEARCHADMINISTRATION
901 South National Avenue, Springfield, MO 65897 • Phone: 417-836-5972 www.missouristate.edu

Appendix C. Complete summary of statistical analyses

ANOVA and post-hoc statistical test data from indicated experiments. In all tables, treatment 1 = LPS or saline control), treatment 2 = UTP (or saline control), P2Y2 = genotype (P2Y2 knockout or wildtype control).

GTT raw data male vs all female:

Within Subjects Effects

Cases	Sum of Squares	df	Mean Square	F	p
RM Factor 1	2.073e +6 [a]	7 [a]	296092.915 [a]	163.275 [a]	< .001 [a]
RM Factor 1 ✻ Treatment 1	76870.823 [a]	7 [a]	10981.546 [a]	6.056 [a]	< .001 [a]
RM Factor 1 ✻ Treatment 2	9500.671 [a]	7 [a]	1357.239 [a]	0.748 [a]	0.631 [a]
RM Factor 1 ✻ Sex	144240.430 [a]	7 [a]	20605.776 [a]	11.363 [a]	< .001 [a]
RM Factor 1 ✻ Treatment 1 ✻ Treatment 2	15825.789 [a]	7 [a]	2260.827 [a]	1.247 [a]	0.277 [a]
RM Factor 1 ✻ Treatment 1 ✻ Sex	16644.303 [a]	7 [a]	2377.758 [a]	1.311 [a]	0.244 [a]
RM Factor 1 ✻ Treatment 2 ✻ Sex	25712.255 [a]	7 [a]	3673.179 [a]	2.026 [a]	0.051 [a]
RM Factor 1 ✻ Treatment 1 ✻ Treatment 2 ✻ Sex	41231.650 [a]	7 [a]	5890.236 [a]	3.248 [a]	0.002 [a]
Residuals	583934.901	322	1813.462		

Note. Type III Sum of Squares

[a] Mauchly's test of sphericity indicates that the assumption of sphericity is violated ($p < .05$).

Raw GTT of female:

Within Subjects Effects

Cases	Sum of Squares	df	Mean Square	F	p
RM Factor 1	1.220e +6 [a]	7 [a]	174284.357 [a]	102.836 [a]	< .001 [a]
RM Factor 1 ✻ Treatment 1	114795.011 [a]	7 [a]	16399.287 [a]	9.676 [a]	< .001 [a]
RM Factor 1 ✻ Treatment 2	16984.032 [a]	7 [a]	2426.290 [a]	1.432 [a]	0.194 [a]
RM Factor 1 ✻ P2Y2	7203.532 [a]	7 [a]	1029.076 [a]	0.607 [a]	0.750 [a]
RM Factor 1 ✻ Treatment 1 ✻ Treatment 2	32683.489 [a]	7 [a]	4669.070 [a]	2.755 [a]	0.009 [a]
RM Factor 1 ✻ Treatment 1 ✻ P2Y2	7828.475 [a]	7 [a]	1118.354 [a]	0.660 [a]	0.706 [a]
RM Factor 1 ✻ Treatment 2 ✻ P2Y2	12505.829 [a]	7 [a]	1786.547 [a]	1.054 [a]	0.395 [a]
RM Factor 1 ✻ Treatment 1 ✻ Treatment 2 ✻ P2Y2	30084.827 [a]	7 [a]	4297.832 [a]	2.536 [a]	0.016 [a]
Residuals	355903.198	210	1694.777		

Note. Type III Sum of Squares

[a] Mauchly's test of sphericity indicates that the assumption of sphericity is violated ($p < .05$).

Normalized GTT male vs female:

Within Subjects Effects

Cases	Sum of Squares	df	Mean Square	F	p
RM Factor 1	189.117[a]	7[a]	27.017[a]	151.471[a]	< .001[a]
RM Factor 1 ✻ Treatment 1	1.505[a]	7[a]	0.215[a]	1.205[a]	0.299[a]
RM Factor 1 ✻ Treatment 2	0.183[a]	7[a]	0.026[a]	0.146[a]	0.994[a]
RM Factor 1 ✻ Sex	19.273[a]	7[a]	2.753[a]	15.437[a]	< .001[a]
RM Factor 1 ✻ Treatment 1 ✻ Treatment 2	1.048[a]	7[a]	0.150[a]	0.839[a]	0.555[a]
RM Factor 1 ✻ Treatment 1 ✻ Sex	1.968[a]	7[a]	0.281[a]	1.576[a]	0.142[a]
RM Factor 1 ✻ Treatment 2 ✻ Sex	0.993[a]	7[a]	0.142[a]	0.796[a]	0.591[a]
RM Factor 1 ✻ Treatment 1 ✻ Treatment 2 ✻ Sex	0.924[a]	7[a]	0.132[a]	0.740[a]	0.638[a]
Residuals	57.432	322	0.178		

Note. Type III Sum of Squares

[a] Mauchly's test of sphericity indicates that the assumption of sphericity is violated ($p < .05$).

Normalized GTT females only:

Within Subjects Effects

Cases	Sum of Squares	df	Mean Square	F	p
RM Factor 1	86.571[a]	7[a]	12.367[a]	81.344[a]	< .001[a]
RM Factor 1 ✻ Treatment 1	2.519[a]	7[a]	0.360[a]	2.367[a]	0.024[a]
RM Factor 1 ✻ Treatment 2	1.085[a]	7[a]	0.155[a]	1.019[a]	0.418[a]
RM Factor 1 ✻ P2Y2	0.742[a]	7[a]	0.106[a]	0.697[a]	0.674[a]
RM Factor 1 ✻ Treatment 1 ✻ Treatment 2	1.192[a]	7[a]	0.170[a]	1.120[a]	0.352[a]
RM Factor 1 ✻ Treatment 1 ✻ P2Y2	0.599[a]	7[a]	0.086[a]	0.563[a]	0.785[a]
RM Factor 1 ✻ Treatment 2 ✻ P2Y2	0.664[a]	7[a]	0.095[a]	0.624[a]	0.736[a]
RM Factor 1 ✻ Treatment 1 ✻ Treatment 2 ✻ P2Y2	1.529[a]	7[a]	0.218[a]	1.437[a]	0.192[a]
Residuals	31.928	210	0.152		

Note. Type III Sum of Squares

[a] Mauchly's test of sphericity indicates that the assumption of sphericity is violated ($p < .05$).

Raw GTT AUC male vs all female:

ANOVA - AUC

Cases	Sum of Squares	df	Mean Square	F	p
Treatment 2	193.694	1	193.694	0.371	0.546
Treatment 1	634.819	1	634.819	1.217	0.276
Sex	30772.237	1	30772.237	58.976	< .001
Treatment 2 ✳ Treatment 1	460.231	1	460.231	0.882	0.353
Treatment 2 ✳ Sex	1239.803	1	1239.803	2.376	0.131
Treatment 1 ✳ Sex	672.734	1	672.734	1.289	0.262
Treatment 2 ✳ Treatment 1 ✳ Sex	1148.048	1	1148.048	2.200	0.145
Residuals	22436.463	43	521.778		

Note. Type III Sum of Squares

Raw GTT AUC all females:

ANOVA - AUC (not norm)

Cases	Sum of Squares	df	Mean Square	F	p
P2Y2	1.942e +7	1	1.942e +7	4.299	0.047
Treatment 1	3.566e +8	1	3.566e +8	78.953	< .001
Treatment 2	560485.381	1	560485.381	0.124	0.727
P2Y2 ✳ Treatment 1	5.211e +6	1	5.211e +6	1.154	0.291
P2Y2 ✳ Treatment 2	17.645	1	17.645	3.906e -6	0.998
Treatment 1 ✳ Treatment 2	5.697e +7	1	5.697e +7	12.611	0.001
P2Y2 ✳ Treatment 1 ✳ Treatment 2	3.029e +7	1	3.029e +7	6.705	0.015
Residuals	1.355e +8	30	4.517e +6		

Note. Type III Sum of Squares

Post Hoc Comparisons - Treatment 1

		Mean Difference	SE	t	p_{tukey}
LPS	Saline	-6275.313	706.236	-8.886	< .001

Note. Results are averaged over the levels of: P2Y2, Treatment 2

Normalized GTT AUC male vs all female:

ANOVA - AUC

Cases	Sum of Squares	df	Mean Square	F	p
Sex	30772.237	1	30772.237	58.976	< .001
Treatment 1	634.819	1	634.819	1.217	0.276
Treatment 2	193.694	1	193.694	0.371	0.546
Sex ∗ Treatment 1	672.734	1	672.734	1.289	0.262
Sex ∗ Treatment 2	1239.803	1	1239.803	2.376	0.131
Treatment 1 ∗ Treatment 2	460.231	1	460.231	0.882	0.353
Sex ∗ Treatment 1 ∗ Treatment 2	1148.048	1	1148.048	2.200	0.145
Residuals	22436.463	43	521.778		

Note. Type III Sum of Squares

Post Hoc Comparisons - Sex

		Mean Difference	SE	t	p_{tukey}
Female	Male	-53.946	7.025	-7.680	< .001

Note. Results are averaged over the levels of: Treatment 1, Treatment 2

Normalized GTT AUC all:

ANOVA - AUC

Cases	Sum of Squares	df	Mean Square	F	p
P2Y2	338.059	1	338.059	1.271	0.269
Treatment 1	33.121	1	33.121	0.125	0.727
Treatment 2	543.775	1	543.775	2.045	0.164
P2Y2 ∗ Treatment 1	513.469	1	513.469	1.931	0.176
P2Y2 ∗ Treatment 2	80.163	1	80.163	0.301	0.587
Treatment 1 ∗ Treatment 2	279.824	1	279.824	1.052	0.314
P2Y2 ∗ Treatment 1 ∗ Treatment 2	371.857	1	371.857	1.398	0.247
Residuals	7180.171	27	265.932		

Note. Type III Sum of Squares

Gene expression:

Muscle GLUT4 male vs all female:

ANOVA - GE Ratio

Cases	Sum of Squares	df	Mean Square	F	p
Sex	4186.769	1	4186.769	7.893	0.128
Treatment 1	4417.757	1	4417.757	8.329	0.097
Treatment 2	162.213	1	162.213	0.306	0.584
Sex ✻ Treatment 1	4245.343	1	4245.343	8.004	0.178
Sex ✻ Treatment 2	489.794	1	489.794	0.923	0.344
Treatment 1 ✻ Treatment 2	498.830	1	498.830	0.940	0.339
Sex ✻ Treatment 1 ✻ Treatment 2	208.729	1	208.729	0.394	0.535
Residuals	16973.871	32	530.433		

Note. Type III Sum of Squares

Muscle GLUT4 by genotype:

ANOVA - GE Ratio

Cases	Sum of Squares	df	Mean Square	F	p
P2Y2	1062.521	1	1062.521	1.550	0.226
Treatment 1	55.457	1	55.457	0.081	0.779
Treatment 2	343.033	1	343.033	0.500	0.486
P2Y2 ✻ Treatment 1	77.844	1	77.844	0.114	0.739
P2Y2 ✻ Treatment 2	1.907	1	1.907	0.003	0.958
Treatment 1 ✻ Treatment 2	1009.313	1	1009.313	1.472	0.237
P2Y2 ✻ Treatment 1 ✻ Treatment 2	172.063	1	172.063	0.251	0.621
Residuals	15769.968	23	685.651		

Note. Type III Sum of Squares

Muscle INSR male vs all female:

ANOVA - GE Ratio

Cases	Sum of Squares	df	Mean Square	F	p
Sex	0.734	1	0.734	0.436	0.514
Treatment 1	3.443	1	3.443	2.046	0.163
Treatment 2	0.030	1	0.030	0.018	0.894
Sex ✻ Treatment 1	0.873	1	0.873	0.519	0.477
Sex ✻ Treatment 2	1.843	1	1.843	1.095	0.304
Treatment 1 ✻ Treatment 2	1.244e -4	1	1.244e -4	7.392e -5	0.993
Sex ✻ Treatment 1 ✻ Treatment 2	0.172	1	0.172	0.102	0.751
Residuals	48.797	29	1.683		

Note. Type III Sum of Squares

Muscle INSR by genotype:

ANOVA - GE Ratio

Cases	Sum of Squares	df	Mean Square	F	p
P2Y2	2.405	1	2.405	1.653	0.216
Treatment 1	0.622	1	0.622	0.428	0.522
Treatment 2	1.164	1	1.164	0.800	0.384
P2Y2 ✻ Treatment 1	0.374	1	0.374	0.257	0.619
P2Y2 ✻ Treatment 2	2.596	1	2.596	1.784	0.199
Treatment 1 ✻ Treatment 2	0.124	1	0.124	0.086	0.773
P2Y2 ✻ Treatment 1 ✻ Treatment 2	0.007	1	0.007	0.005	0.945
Residuals	24.731	17	1.455		

Note. Type III Sum of Squares

Adipose GLUT4 male vs all female:

ANOVA - GE Ratio

Cases	Sum of Squares	df	Mean Square	F	p
Sex	0.835	1	0.835	1.413	0.243
Treatment 1	1.935	1	1.935	3.276	0.380
Treatment 2	0.375	1	0.375	0.635	0.431
Sex ✻ Treatment 1	0.005	1	0.005	0.009	0.924
Sex ✻ Treatment 2	0.016	1	0.016	0.027	0.870
Treatment 1 ✻ Treatment 2	0.728	1	0.728	1.232	0.275
Sex ✻ Treatment 1 ✻ Treatment 2	0.037	1	0.037	0.062	0.804
Residuals	18.901	32	0.591		

Note. Type III Sum of Squares

Adipose GLUT4 by genotype:

ANOVA - GE Ratio

Cases	Sum of Squares	df	Mean Square	F	p
Treatment 1	1.524	1	1.524	2.977	0.499
Treatment 2	0.001	1	0.001	0.003	0.958
P2Y2	2.111	1	2.111	4.122	0.355
Treatment 1 ✻ Treatment 2	0.628	1	0.628	1.226	0.281
Treatment 1 ✻ P2Y2	0.666	1	0.666	1.300	0.267
Treatment 2 ✻ P2Y2	4.263	1	4.263	8.325	0.279
Treatment 1 ✻ Treatment 2 ✻ P2Y2	1.033	1	1.033	2.017	0.170
Residuals	10.753	21	0.512		

Note. Type III Sum of Squares